

OPEN ACCESS

EDITED BY
Gisele Cristina Favero,
Universidade Federal de Minas Gerais, Brazil

REVIEWED BY
Neeraj Kumar,
National Institute of Abiotic Stress
Management (ICAR), India
Dr. D. K. Meena,
Central Inland Fisheries Research Institute
(ICAR). India

*CORRESPONDENCE
Abdallah Tageldein Mansour
amansour@kfu.edu.sa
Yasmina M. Abd-Elhakim
yasmina.forensic@gmail.com

RECEIVED 05 September 2025 ACCEPTED 31 October 2025 PUBLISHED 21 November 2025

CITATION

Behairy A, El-Houseiny W, Mansour AT, Abd-Elhakim YM, Alsaqufi AS, Alkhamis YA, Hassanien HA and Abd-Allah NA (2025) Dietary α-sitosterol mitigates titanium dioxide nanoparticle-induced hemato-immunotoxicity, oxidative stress, and gene expression dysregulation in *Oreochromis niloticus*. *Front. Mar. Sci.* 12:1700010. doi: 10.3389/fmars.2025.1700010

COPYRIGHT

© 2025 Behairy, El-Houseiny, Mansour, Abd-Elhakim, Alsaqufi, Alkhamis, Hassanien and Abd-Allah. This is an open-access article distributed under the terms of the Creative Commons Attribution License (CC BY). The use, distribution or reproduction in other forums is permitted, provided the original author(s) and the copyright owner(s) are credited and that the original publication in this journal is cited, in accordance with accepted academic practice. No use, distribution or reproduction is permitted which does not comply with these terms.

Dietary α-sitosterol mitigates titanium dioxide nanoparticle-induced hemato-immunotoxicity, oxidative stress, and gene expression dysregulation in *Oreochromis niloticus*

Amany Behairy¹, Walaa El-Houseiny², Abdallah Tageldein Mansour^{3*}, Yasmina M. Abd-Elhakim^{4*}, Ahmed Saud Alsaqufi³, Yousef Ahmed Alkhamis³, Hesham A. Hassanien³ and Noura A. Abd-Allah⁵

¹Department of Physiology, Faculty of Veterinary Medicine, Zagazig University, Zagazig, Egypt, ²Department of Aquatic Animal Medicine, Faculty of Veterinary Medicine, Zagazig University, Zagazig, Egypt, ³Animal and Fish Production Department, College of Agricultural and Food Sciences, King Faisal University, Al-Ahsa, Saudi Arabia, ⁴Department of Forensic Medicine and Toxicology, Faculty of Veterinary Medicine, Zagazig University, Zagazig, Egypt, ⁵Department of Clinical Pathology, Faculty of Veterinary Medicine, Zagazig University, Zagazig, Egypt

Introduction: Titanium dioxide nanoparticles (TDNPs) are widely used in food industries, agricultural and consumer products, and diagnostic purposes, leading to their potential release into aquatic environments and associated physiological risks to non-target aquatic organisms, particularly fish. α -Sitosterol (STL), a phytosterol, acts by enhancing antioxidant defenses and modulating inflammatory signaling pathways. Hence, this study investigated whether dietary STL can protect Nile tilapia (*Oreochromis niloticus*) from TDNPs-induced toxicity during a 60-day exposure.

Methods: In this study, 300 Nile tilapia were allocated into four groups. The control group received a basal diet, the STL group was fed a diet supplemented with 80 mg STL/kg, the TDNPs group was exposed to 10 mg/L of TDNPs in water, and the TDNPs + STL group was exposed to TDNPs and fed the STL-supplemented diet. Results: Dietary STL supplementation markedly improved growth performance, with increases of 33%-60% in final body weight, weight gain, and daily growth rate, and a 29% reduction in feed conversion ratio compared to TDNPs-exposed fish. STL supplementation also restored hematological parameters altered by TDNPs exposure, including significant recovery of red blood cells, hemoglobin, packed cell volume, and white blood cells, thereby reversing macrocytic normochromic anemia and leukopenia. Furthermore, STL significantly decreased elevated serum alanine aminotransferase, aspartate aminotransferase, alkaline phosphatase, urea, and creatinine levels induced by TDNPs, and normalized lipid profiles by reducing total cholesterol, triglycerides, and low-density lipoprotein cholesterol, while elevating high-density lipoprotein cholesterol. STL-fed fish also exhibited significant reductions in stress biomarkers (glucose and cortisol) and enhanced

innate immune responses, as evidenced by higher lysozyme, complement 3, nitric oxide, nitro blue tetrazolium, and phagocytic activity. Antioxidant status was strengthened through increased superoxide dismutase, catalase, and glutathione peroxidase activities and reduced malondialdehyde levels. At the molecular level, STL supplementation downregulated endoplasmic reticulum stress-related genes (chop, jnk, xbp-1, and perk), while upregulating autophagy-related genes (beclin-1 and lc3-ii) and downregulating mtor and p62. Histological analysis confirmed STL's protective effects, showing marked recovery of intestinal, hepatic, renal, and splenic structures.

Conclusion: These findings demonstrated that STL confers multi-level protection against TDNPs-induced oxidative, metabolic, and cellular stress, highlighting its potential as a functional dietary supplement for mitigating nanotoxicity in aquaculture.

KEYWORDS

titanium dioxide nanoparticles, alpha sitosterol, oreochromis niloticus, oxidative stress, endoplasmic reticulum stress, autophagy, gene expression, immunity

1 Introduction

Nanoparticles (NPs) are increasingly used in agriculture and aquaculture due to their potential to improve food security and resource efficiency (Alam et al., 2024; Khan et al., 2024). However, their release into aquatic environments raises environmental and ecotoxicological concerns, particularly for non-target organisms such as fish (Ameen et al., 2021; Min et al., 2023; Atanda et al., 2025). Titanium dioxide nanoparticles (TDNPs) rank among the most produced and extensively utilized nanomaterials across agriculture, consumer products, and environmental sectors (Sungur, 2021). In agriculture, they are experimentally applied as nanofertilizers, photocatalytic agents for pesticide degradation, and antimicrobial coatings to enhance plant growth and protect crops from pathogens (Lyu et al., 2017; Ko and Hwang, 2019; Rodríguez-González et al., 2019). Moreover, TDNPs have been experimentally explored in aquaculture for various purposes, including photocatalytic water disinfection and anti-infective applications (Alexpandi et al., 2020) and degradation of antibiotic residues in aquaculture wastewater in the Mekong Delta, Vietnam (Do et al., 2019). Yet, accidental environmental release of TDNPs can result in bioaccumulation in plankton and transfer through the food web, posing risks to multiple trophic levels (Abdel-Latif et al., 2020; Rashid et al., 2021). Field measurements indicate TDNPs levels in contaminated waters ranging from 1 to 200 µg/L near industrial sites, highlighting the potential for environmental exposure (Kiser et al., 2009; Kozliak and Paca, 2012; Maiga et al., 2019; Liu et al., 2022).

Exposure to TDNPs has been shown to induce physiological, immunological, and histological disturbances in fish. For instance, increased activities of liver enzymes such as alkaline phosphatase (ALP), alanine aminotransferase (ALT), and aspartate

aminotransferase (AST) have been reported in Clarias gariepinus exposed to 1-10 mg/L TDNPs (Tunçsoy, 2021). Immunotoxic effects, including lysosomal destabilization and impaired phagocytosis, were observed in fathead minnows (Pimephales promelas) following intraperitoneal TDNPs injection (10 µg/g b.wt) (Jovanović et al., 2015). In neotropical detritivorous fish (Prochilodus lineatus), 1-50 mg/L TDNPs exposure for 14 days reduced red blood cell (RBC), white blood cell (WBC), and lymphocyte counts (Carmo et al., 2019). Histopathological changes in the intestine and liver were reported in Nile tilapia (Oreochromis niloticus) exposed to 1 mg/L TDNPs for 21 days (De Silva and Pathiratne, 2023), while biochemical and tissue alterations were also observed in Danio rerio fed 200 µg/g TDNPs for 14 days (Cunha and De Brito-Gitirana, 2020). Oxidative stress from reactive oxygen species (ROS) is a key mechanism underlying these effects (Vineetha et al., 2021). TDNPs can further disrupt endoplasmic reticulum (ER) function, activating ER stress pathways and autophagy, contributing to cellular damage (Zhou et al., 2024, 2025).

Despite various reports on TDNPs-induced toxicity in fish, little is known about dietary strategies that could mitigate these harmful effects, especially in commercially important species such as Nile tilapia (*O. niloticus*) (Vineetha et al., 2021). Nile tilapia is one of the most widely cultivated aquaculture species globally, ranking as the third-most significant in aquaculture, due to its fast growth, broad environmental tolerance, high feed conversion, and ease of reproduction in captivity (FAO, 2022; Geletu and Zhao, 2023). In 2013, the global production of tilapia reached 4.8 million tons, with Nile tilapia accounting for over 70% of this total (McAndrew et al., 2016). Egypt is a leading producer of Nile tilapia, with production estimates varying by source and year; recent reports indicate an output exceeding 1.1 million tons in 2023, while earlier figures reached approximately 1.6 million tons in 2021, positioning Egypt

as the largest producer in Africa and the third largest globally, after China and Indonesia (El-Sayed, 2021; Alliance, 2023). Additionally, because of its biological suitability as a model species for toxicological and nutritional research, Nile tilapia serves as an ideal tropical fish model for evaluating various forms of nanotoxicity including TDNPs (Perera and Pathiratne, 2014; De Silva and Pathiratne, 2023; Ribeiro et al., 2025).

Phytosterols possess a broad spectrum of physiological activities, comprising anti-inflammatory, antioxidant, immunomodulatory, and antimicrobial effects, along with protective roles in gut and liver health (Feng et al., 2020). They are known to reduce cholesterol absorption and lower low-density lipoprotein cholesterol (LDL-C) levels (Li et al., 2022), thereby contributing to improved growth performance in animals (Ding et al., 2021). Moreover, phytosterols can decrease malondialdehyde (MDA) concentrations while enhancing the antioxidant enzyme activities comprising superoxide dismutase (SOD) and glutathione peroxidase (GPx) (Abdel-Moneim et al., 2020). Among these, α-sitosterol (α-STL), a bioactive phytosterol produced by Streptomyces misakiensis, has demonstrated promising biological properties (Abdelaziz et al., 2024). Dietary supplementation with phytosterols has been shown to elevate immunoglobulin levels and upregulate the mRNA expression of immune-related markers, including interleukin-10 and β-defensin in gilthead seabream (Sparus aurata) (Costas et al., 2014). β-Sitosterol (β-STL) specifically exhibits notable in vitro anti-apoptotic and antiinflammatory effects by downregulating caspase-3 and interleukin-1β, while upregulating B-cell lymphoma-2 (Bcl-2) expression (Fan et al., 2023). Furthermore, β-STL mitigated cerebral injury by modulating pathways associated with ER stress, cholesterol overload, and neuronal apoptosis (Tang et al., 2024). Dietary supplementation with α -STL at 80 mg/kg for 60 days enhanced antioxidant status and growth performance, strengthened the immune response, and regulated gene expression in Nile tilapia following Candida albicans infection (El-Houseiny et al., 2025), highlighting its potential as a protective dietary intervention against cellular stress and toxicity.

Based on the aforementioned STL biological activities, we hypothesized that it could mitigate TDNPs impacts in tilapia. Therefore, the present study aimed to (i) investigate the toxic effects of TDNPs on growth, hematobiochemical parameters, stress responses, immune status, antioxidant defenses, ER stress, autophagy, and tissue histopathology in Nile tilapia, and (ii) evaluate the potential protective role of STL supplementation in mitigating TDNPs-induced adverse effects. To our knowledge, this work represents the first *in vivo* investigation of the protective efficacy of STL against TDNPs toxicity in Nile tilapia.

2 Materials and methods

2.1 Tested chemicals

TDNPs (99.98% purity and molecular weight 79.87 g/mol) were obtained from Alpha Chemica, Mumbai, India. The same batch of TDNPs was previously characterized by one of the current authors

(Abd-Elhakim et al., 2023). Characterization revealed that the particles had a uniform spherical morphology with a primary size distribution ranging from 6 to 19 nm, as determined by transmission electron microscopy. X-ray diffraction analysis confirmed the rutile crystalline structure, while dynamic light scattering showed a hydrodynamic diameter of approximately 12 nm. The zeta potential was measured at -25 mV, indicating moderate stability in suspension. To maintain dispersion and minimize aggregation during exposure, the TDNPs suspensions were sonicated for 15 min before use and kept under continuous mild aeration and stirring in the stock solution.

 α -STL used in this study was derived from *S. misakiensis*, as previously isolated, identified, and characterized in El-Houseiny et al. (2025), following the protocol described by Abdelaziz et al. (2024). Sigma-Aldrich Co. of St. Louis, Missouri, USA, supplied all of the analytical grade chemicals and reagents used in this study.

2.2 Experimental fish

The male Nile tilapia fingerlings (an average body weight of 11.79 ± 0.33 g) were obtained from the Fish Research Centre at Zagazig University, Egypt. Prior to the trial, the fish were acclimated in a laboratory environment, housed in glass aquariums containing 70 L of dechlorinated tap water, and fed a basic diet to minimize external stress factors.

Throughout the trial, key water quality parameters in the aquariums, including pH, dissolved oxygen, water temperature, and ammonia, were regularly monitored using an automated Hanna HI-9147 probe and ammonia test kits (HACH, HACH Co., Loveland, CO, USA). Water parameters were maintained within optimal ranges through continuous aeration, thermostatically controlled heaters, and daily monitoring to ensure uniform environmental conditions across all tanks. Tanks were positioned to avoid direct light and drafts, and water circulation was standardized using identical aeration setups. All parameters remained stable and within the optimal ranges for fish husbandry, as recommended by Boyd and Tucker (2012), with mean \pm SD values as follows: pH at 6.5 \pm 0.5, temperature at 27.3 \pm 0.05 °C, ammonia concentration at 0.03 ± 0.01 mg/L, and dissolved oxygen at 6.80 ± 0.5 mg/L. A controlled photoperiod of 12 h of light and 12 h of dark was maintained throughout the study. The experiment was conducted under the regulation of Zagazig University's Animal Use in Research Committee (approval number ZU-IACUC/2/F/85/2025), adhering to the ethical guidelines of the National Institutes of Health (NIH) for the Care and Use of Laboratory Animals in Scientific Research.

2.3 Formulation of diet and experimental plan

In accordance with the Nutrient Requirements of Fish and Shrimp (Jobling, 2012), the ingredients for the experimental diet presented in Table 1 were formulated to adequately fulfill the dietary needs of the fish. The diet's ingredients were thoroughly

TABLE 1 Ingredients and proximate chemical analysis of the experimental diets (g/kg diet, on a dry matter basis).

Ingredients	Control	STL	
Fish meal	110	110	
Soybean meal	420	420	
Ground corn	240	240	
Wheat bran	100	100	
Corn oil	40	40	
Starch	40	39.92	
α-Sitosterol (STL)	-	0.08	
Cod liver oil	20	20	
Mineral and Vitamin premix ¹	30	30	
Chemical analysis			
Crude protein (N×6.25)	308.8	308.8	
Crude lipids	75.0	75.0	
Crude fiber	52.8	52.8	
Ash	72.2	72.23	
Nitrogen-free extract ²	491.2	491.1	
Gross energy (kcal kg ⁻¹) ³	4,472	4,472	

¹Vitamin and mineral premix (Agri-Vet, 10th Ramadan city, Egypt; per kg of diet) provides: vitamin D3–600 IU, vitamin A 4,000 IU, vitamin E 20 mg, vitamin B1 3.6 mg, vitamin K3–5 mg, vitamin B2–6 mg, vitamin B3 14.4 mg, vitamin B5–12 mg, vitamin B12 0.02 mg, vitamin B6 3.5 mg, folic acid 0.9 mg, biotin 0.07 mg, vitamin C 50 mg, inositol 300 mg, Fe 30 mg, Mg 15 mg, Cu 4 mg, Zn 42 mg, Co 0.11 mg, K 75 mg, Se 0.04 mg, Mn 1.6 mg, I 0.4 mg, and Mo 0.005 mg.

mixed before being processed into pellets, air-dried for 24 h at ambient temperature, and subsequently kept at 4 °C until needed. In line with the AOAC (2006) guidelines, the crude protein, moisture, crude fat, crude fiber, and total ash content of each diet investigated were analyzed using the forced-air oven, macro-Kjeldahl method, ether extraction technique, and muffle furnace, respectively.

During the acclimation and experimental phases, fish were provided with a basal diet equivalent to 3% of their body weight per day. Feeding was conducted twice daily at 09:00 and 16:00; such time points were selected based on the diurnal feeding behavior of Nile tilapia. These time points were chosen because tilapia exhibit peak feeding activity during the mid-morning and mid-afternoon under standard photoperiods, which optimizes feed intake efficiency and growth performance in fingerlings (Souza et al., 2014; Hamed et al., 2024). Fish were fed to apparent satiation to ensure adequate nutrient intake without overfeeding. The feeding amount was adjusted biweekly based on changes in biomass, which was determined by sampling and weighing a representative subset of fish from each group. To maintain optimal water quality and minimize the accumulation of waste, uneaten feed and feces were removed daily using a siphoning method. Additionally, 50% of the water in each tank was replenished every other day using preaerated and temperature-matched dechlorinated tap water to avoid inducing stress due to sudden environmental changes.

After acclimation, 300 fish were randomly assigned to four treatment groups, with each group containing 75 fish. Each treatment was further divided into five replicates of 15 fish per replicate. The first group (Control) was sustained in clean glass aquariums and was given a basic diet without any additives. The second group (STL) was also housed in clean glass aquariums and was provided with diets that included 80 mg/kg STL. The selected STL dose was based on the findings of El-Houseiny et al. (2025), who performed a full gradient (0, 20, 40, 60, and 80 mg/kg) and found maximal growth, antioxidant, and immune benefits at 60-80 mg/kg; thus, the highest effective dose was chosen. The third group (TDNPs) was exposed to TDNPs at a concentration of 10 mg/L. This exposure level reflects an environmentally relevant sublethal concentration validated by Vineetha et al. (2021) over 14 days to mimic realistic exposure scenarios in aquaculture effluents and demonstrated clear biochemical and histopathological endpoints. The fourth group (STL + TDNPs) received STL and was also exposed to TDNPs at the previously specified levels. To ensure stable concentration and homogeneity, and to minimize fluctuations in TDNPs exposure levels, 50% of the tank water was replaced daily with well-aerated water containing freshly prepared TDNPs suspensions. Exposures were performed for 60 days. All experimental procedures, including feeding, sampling, and measurements, were conducted in a blinded manner. Investigators responsible for outcome measurements were blinded to group allocations, with fish tanks, diets, and sample containers coded to prevent observer bias during assessments of growth, hematological, biochemical, molecular, and histopathological endpoints.

2.4 Blood and tissue sampling collection

After the experimental period, fish were anesthetized with 100 mg/L benzocaine solution (Al-Nasr Pharmaceutical Chemicals Co., Oubour, Qalyubia, Egypt). Previous studies in Nile tilapia have demonstrated that immersion in benzocaine at 100 mg/L induces stage III anesthesia within 2-3 min and full recovery within 5-7 min, thereby minimizing handling stress and avoiding significant alterations in hematological and physiological parameters (Okamura et al., 2010; Weinert et al., 2015). Approximately 0.5 mL of blood was collected from the caudal vein of each fish using a sterile 3-mL syringe fitted with a 24-gauge needle. Three separate batches of blood samples were collected, totaling 15 samples per group (3 samples per replicate). The first batch was obtained in EDTA tubes for blood cell count analysis. The second batch was collected in heparinized tubes for evaluating phagocytic and respiratory burst activities. The third batch was collected in plain tubes (without anticoagulants), allowed to clot at room temperature, and then centrifuged at 664 ×g for 15 min to obtain serum, which was stored at -20°C for subsequent biochemical analyses. Following blood collection, fish were euthanized by an overdose of benzocaine solution (250 mg/L) (Neiffer and Stamper, 2009). Liver tissues were collected from 15 fish per group (three samples per replicate), thoroughly trimmed of connective tissue and fat, rinsed

²Calculated by difference (100 - protein% + lipids% + ash% + crude fiber%).

 $^{^3}$ Gross energy (GE) was calculated as 5.65, 9.45, and 4.11 kcal/g for protein, lipid, and NFE, respectively.

with chilled 0.9% saline, and blotted dry. The liver samples were homogenized in 10 volumes of phosphate-buffered saline (pH 7.4). The hepatic homogenate underwent a gentle centrifugation at $664 \times g$ for 15 min in a chilled centrifuge set to 4°C. After separation, the clear supernatant was carefully collected and preserved at -80°C until assessing oxidative and antioxidant indicators.

For gene expression analysis, an additional 15 liver samples per group (3 samples per replicate) were preserved in TRIzol reagent (Thermo Scientific, USA) and stored at -80°C for RNA extraction to assess ER stress- and autophagy-related genes. Furthermore, liver, spleen, anterior intestine, and anterior kidney samples were randomly collected from 15 fish per group (3 samples per replicate) and fixed in 10% neutral buffered formalin for histopathological investigation. All tissue sample analyses were performed in a blinded manner, with sample identity coded to prevent bias during evaluation. The sample allocation and number of fish tested for each parameter within the experimental groups are demonstrated in Supplementary Figure S1.

2.5 Growth performance analysis

At the beginning and end of the feeding trial, the initial body weight (IBW) and final body weight (FBW) of the fish were recorded. Growth performance indices were then calculated following the equations of Jobling (1995), including:

Survival Rate(%)

= (Number of fish at the beginning of the experiment/ $Number of fish at the end of the experiment) \times 100$

Weight Gain (WG, g) = FBW – IBW

Daily Weight Gain (DWG, g/day) = WG/60 days

Specific Growth Rate (SGR, %/day) = $[(\ln FBW - \ln IBW)/60 \text{ days}] \times 100$

Feed Intake (FI, g feed/fish)

= Total feed consumed/Number of fish per aquarium

Feed Conversion Ratio (FCR) = Total FI/Total WG

Condition Factor = $(W/L^3) \times 100$ where W = body weight(g) and L = total length(cm)

2.6 Assessment of hematological indices

Hematological indices, including WBC count, RBC count, hematocrit, and hemoglobin (Hb) concentration, were assessed

following the method defined by Bain et al. (2016). Additionally, mean corpuscular volume (MCV) percentage, mean corpuscular hemoglobin (MCH), and packed cell volume (PCV) were measured by the microhematocrit technique (Hrubec et al., 2000). Methanol-fixed blood smears were Wright–Giemsa-stained to analyze the differential leukocyte count. Leukocytes were identified and classified based on morphological characteristics such as nuclear shape, cytoplasmic granules, and cell size, following the criteria described by Hrubec et al. (2001). All hematological assays were previously validated for use in *O. niloticus* and other tilapia species, ensuring methodological reliability (Hrubec et al., 2000; Sayed and Moneeb, 2015; Bain et al., 2016). To confirm intra-assay precision, 10% of randomly selected samples were analyzed in duplicate, yielding a mean coefficient of variation (CV) of <5% across all hematological parameters.

2.7 Hepatorenal function indicators, lipid profile, and stress markers

To evaluate various biochemical markers in serum, specific enzymatic and colorimetric assays were conducted using commercially available Spinreact kits (Esteve De Bas, Girona, Spain) consistent with the manufacturer's instructions. ALT activity was measured using the Spinreact kit, catalog no. BEIS45-E. The assay is based on ALT catalyzing the transamination of alanine and α-ketoglutarate to form glutamate and pyruvate. Pyruvate is then converted to lactate by lactate dehydrogenase (LDH) and NADH. The decrease in NADH absorbance at 340 nm, monitored photometrically, reflects ALT activity, according to Murray and Kaplan (1984a). AST activity was determined using the Spinreact kit, catalog no. BEIS46-E. In this assay, an amino group is reversibly transferred from aspartate to α -ketoglutarate, forming oxaloacetate and glutamate. The resulting oxaloacetate is then converted into malate through the action of malate dehydrogenase (MDH), a reaction that concurrently involves the oxidation of NADH. The decline in NADH absorbance at 340 nm corresponds to AST activity, following the method described by Murray and Kaplan (1984b). ALP activity was assessed with the Spinreact kit, catalog no. MDBEIS44-I. The assay depends on ALP's hydrolysis of p-nitrophenyl phosphate to 4-nitrophenoxide, which generates a yellow color measurable photometrically at 405 nm. The yellow color intensity is proportionate to ALP activity, as detailed by Wenger et al. (1984). Serum creatinine levels were determined by the Spinreact kit, catalog no. MDBSIS13-E. The assay is based on creatinine reacting with sodium picrate to form a red complex, which is quantifiable at 505 nm, per the method of Fossati et al. (1983). Urea concentration was estimated by the Spinreact kit, catalog no. BSIS35-I, which is based on the reaction with o-phthalaldehyde in an acidic medium, forming a chromogenic complex measurable at 510 nm, as defined by Kaplan (1984).

Serum cholesterol and triglyceride concentrations were assessed using Spinreact kits (catalog nos. TKBSIS48-I and MXBSIS49-I), following the methods of Allain et al. (1974) and Fossati and Prencipe (1982), respectively. The serum levels of high-density

lipoprotein cholesterol (HDL-C) and LDL-C were measured by colorimetric Biodiagnostic kits (catalog nos. CH 12–30 and CH 12 31, respectively) per the protocols of Lopes-Virella et al. (1977) and Assmann et al. (1984), respectively. Serum cortisol concentrations were assessed by a commercial ELISA (enzyme-linked immunosorbent assay) kit (MyBioSource Inc., San Diego, CA, USA; catalog no. MBS704055), while serum glucose amounts were determined colorimetrically via a kit from the same provider (catalog no. MBS169259).

All biochemical assays were validated for fish serum applications and cross-referenced with studies on *O. niloticus* and related species (Dawood et al., 2020; Zahran et al., 2021; Reda et al., 2025). Analytical reproducibility was confirmed by duplicate analysis of 10% of samples, with intra-assay and inter-assay CVs of <6% and <8%, respectively.

2.8 Serum immune parameters

The assessment of complement 3 (C3) levels in fish serum was performed by MyBioSource Co. kits (California, USA), based on the company's directives (catalog no. MBS281020). C3 concentrations were measured by a two-site sandwich ELISA. Wells pre-coated with a C3-specific antibody captured C3 from samples and standards. After washing, a biotin-conjugated C3 antibody was added, followed by streptavidin-HRP. Substrate was then applied, producing a color proportional to C3 concentration, which was measured at 450 nm after stopping the reaction.

Total nitric oxide (NO) production was assessed by a colorimetric kit from MyBioSource (catalog no. MBS480450) via reducing nitrate to nitrite via the NADH-dependent enzyme nitrate reductase. The generated nitrite was then quantified by the Griess reagent (Bryan and Grisham, 2007). The final reaction product was detected spectrophotometrically at 540 nm. Serum lysozyme activity was determined using the turbidimetric method described by Ellis (1999) with a suspension of *Micrococcus lysodeikticus* (0.2 mg/mL) prepared in 0.05 M phosphate-buffered saline (PBS) (pH 6.2). A mixture containing 0.75 mL of the *M. lysodeikticus* suspension and 0.25 mL of serum was incubated for 5 min at 25 °C. The decrease in optical density at 540 nm was recorded every minute using a 5010 Photometer (BM Co., Germany). Lysozyme activities were calculated based on a standard curve of serially diluted chicken egg white lysozyme (Sigma, USA).

Leukocyte phagocytic activity in fish blood was measured following Siwicki et al. (1994). Whole blood was diluted with PBS, and leukocytes were enumerated and adjusted to a final concentration of 1×10^6 cells/mL. Yeast cells, previously coated to enhance recognition, were mixed with the leukocyte suspension at a 1:100 ratio. The mixture was then left to incubate for 30 min at 25 °C. After incubation, the cells were stained and examined under a microscope, enabling the identification and quantification of those actively engaged in phagocytosis. In parallel, the cells' respiratory burst activity was measured using the nitro blue tetrazolium (NBT) reduction method, following the approach outlined by Rook et al. (1985). Leukocytes $(1 \times 10^6 \text{ cells/mL})$ were incubated with NBT and

phorbol myristate acetate at 25 °C for 30 min. Formazan-positive cells were counted microscopically, and formazan was also quantified spectrophotometrically at 620 nm after dissolving in dimethyl sulfoxide.

All immune assays were validated for the tilapia species as previously reported (Dawood et al., 2020; Zahran et al., 2021). Intraassay and inter-assay CVs were <6% and <8%, respectively, confirming high reproducibility of the immune biomarker assessments.

2.9 Assessment of the hepatic homogenate oxidative stress markers

Hepatic MDA levels were quantified by commercial kits from Biodiagnostic Co. (Cairo, Egypt, catalog no. MD 25 29), following the scheme established by Mihara and Uchiyama (1978). This assay measures thiobarbituric acid reactive substances (TBARS), with MDA concentration serving as the indicator of lipid peroxidation. Catalase (CAT) activity in liver supernatants was determined by Biodiagnostic kits (catalog no. CA 25 17) based on Aebi (1984). The assay monitors the decomposition of hydrogen peroxide by CAT, tracking the decrease in absorbance at 240 nm as a measure of enzymatic activity. SOD activity in liver tissues was assessed using Biodiagnostic kits (catalog no. SD 25 21), following the approach of Nishikimi et al. (1972). This process relies on SOD's capacity to hinder the phenazine methosulfate-driven reduction of nitroblue tetrazolium, thereby quantifying enzymatic activity. For GPx, the EnzyChrom TM Glutathione Peroxidase Assay Kit (EGPX-100) from Bio-Assay Systems (California, USA) was employed, based on the protocol by Paglia and Valentine (1967). This colorimetric assay measures the consumed nicotinamide adenine dinucleotide phosphate in enzyme-coupled reactions, with the reduction in absorbance at 340 nm reflecting the sample GPx activity. Assay validation and performance were confirmed according to manufacturer-provided quality controls, with recovery rates between 95% and 104% and CVs below 6%. The applicability of these oxidative stress assays to O. niloticus has been documented in previous studies (Abdel-Khalek et al., 2015; Soror et al., 2021; El-Naby et al., 2025).

2.10 Hepatic endoplasmic stress and autophagy-related gene analysis

Frozen liver tissues (100 mg) were homogenized in 1 mL of TRIzol reagent, and total RNA was subsequently isolated using the easyREDTM extraction kit (iNtRON Biotechnology, Korea), following the producer's procedure. The extracted RNA was then transformed into first-strand cDNA by the QuantiTect[®] Reverse Transcription Kit (Qiagen, Germany). Based on the accession numbers listed in Supplementary Table S1, primer sequences of ER stress-related genes [C/EBP homologous protein (*chop*), c-Jun N-terminal kinase (*jnk*), X-box binding protein-1 (*xbp-1*), and protein kinase R-like ER kinase (*perk*)] and autophagy-related genes [*beclin-1* and light chain 3 phosphatidylethanolamine

conjugate (lc3-ii), mammalian target of rapamycin (mtor), and p62] were designed by the NCBI Primer-BLAST tool (https:// www.ncbi.nlm.nih.gov/tools/primer-blast/). The method of Sreedharan et al. (2018) was used to assess the efficiency of the primer. Using the QuantiTect® SYBR® Green PCR kit (Qiagen, Germany), amplification was carried out on a Rotor-Gene Q thermocycler under the following thermal profile: the reaction began with an initial denaturation at 95°C for 10 min, then proceeded through 40 amplification cycles involving denaturation at 95°C (15 s), annealing at 60°C (30 s), and extension at 72°C (30 s). The reference gene was selected based on the approach described by Rojas-Hernandez et al. (2019). To assess expression stability across the experimental groups, three housekeeping genes were evaluated: glyceraldehyde-3-phosphate dehydrogenase (gapdh), \(\beta \)-actin, and elongation factor 1- α (*ef-1-\alpha*). Among them, *act-\beta* showed the most stable expression and was therefore chosen as the reference gene. The $2^{-\Delta\Delta CT}$ approach, outlined by Livak and Schmittgen (2001), was adopted to evaluate the relative expression levels of the mRNA profiles for every gene.

2.11 Histopathological study

Intestinal, hepatic, renal, and splenic tissues were placed in 10% formalin for 48 h, subjected to a dehydration process using varying gradations of ethyl alcohol, cleansed in xylene, and subsequently embedded in paraffin blocks, which were then sliced with a microtome to 5-µm sections. The sections were stained with hematoxylin-eosin to facilitate histopathological evaluation (Suvarna et al., 2018). Five non-overlapping fields per organ per fish were randomly selected for analysis blindly by a pathologist using a 10× objective lens. Following the methodology outlined by Bernet et al. (1999), histopathological alterations observed in the liver (including degeneration, necrosis, inflammatory infiltration, and edema), kidney (such as interstitial edema, inflammatory cell infiltration, and glomerular shrinkage), and spleen (characterized by hypocellularity of the white pulp, sinusoidal dilation, and hemosiderin deposition) were evaluated across all experimental fish groups, as summarized in Supplementary Table S2. Histopathological changes were evaluated using a scoring system, and the average score was determined for each fish. Scores ranged from 0 (no observable alteration) to 4 (widespread lesion), indicating the severity of the changes.

2.12 Statistical analysis

To confirm that the data satisfied the homogeneity and normality assumptions, the Kolmogorov–Smirnov and Levene's tests were applied prior to analysis of variance (ANOVA). A one-way ANOVA followed by Tukey's multiple comparison test was performed to detect significant differences among treatments at the end of the experiment. Tukey's test incorporates an error correction procedure to reduce false positives across multiple pairwise

comparisons. Since the histopathological scoring data did not meet the assumptions required for parametric analysis, they were evaluated using the Kruskal–Wallis test followed by Dunn's post hoc test with Bonferroni-adjusted p-values to minimize Type I error. Results are presented as mean \pm standard error (SE), with statistical significance set at p < 0.05. All statistical analyses were performed using IBM SPSS Statistics software, version 11.0 (IBM Corp., Armonk, NY, USA), and all figures were constructed using GraphPad Prism software, version 9.0 (GraphPad Software, San Diego, CA, USA).

3 Results

3.1 Impact on the growth performance of fish

The effects of incorporating STL into the diet of O. niloticus and exposure to TDNPs over 60 days are summarized in Table 2. While both the control and TDNPs-exposed groups showed increases in body weight at the end of the experiment, the TDNPs group exhibited significantly (p < 0.05) lower growth performance compared to the control. Specifically, fish exposed to TDNPs had a 24.74% lower FBW and condition factor (13.68%), along with significant reductions in WG (40.80%), DWG (40%), SGR (28.99%), and FI (16.55%). Additionally, the FCR was highest in the TDNPs group (increased by 41.10%) among all treatments. Moreover, the TDNPs-exposed fish showed significantly (p < 0.05) reduced survival by 20% compared to the control group. In contrast, STL supplementation significantly (p < 0.05) improved FBW (33.33%), WG (58.01%), DWG (60%), SGR (32.61%), FI (12.76%), and condition factor (10.26%), while reducing the FCR by 28.77% compared to the control group. Notably, the STL + TDNPs group showed significantly higher survival, condition factor, WG, and DWG, and lower FCR compared to the TDNPs group (p < 0.05).

3.2 Effects on hematological indices

Exposure of the fish to water contamination by TDNPs for 60 days led to a significant reduction (p < 0.05) in levels of RBCs (45.16%), HB (33.54%), PCV (28.94%), WBCs (36.79%), heterophils (32.74%), lymphocytes (30.99%), eosinophils (35.48%), and monocytes (56.98%), while MCV (29.60%) and MCH (21.44%) increased when compared to the control fish (Table 3). There was no significant change in MCHC between the treated groups (p > 0.05). The observed increase in MCV and MCH, along with a normal MCHC in the TDNPs group, indicated macrocytic normochromic anemia. In contrast, STL supplementation led to a significant (p < 0.05) increase in RBC (11.06%), PCV (5.34%), and lymphocyte (3.76%) levels compared to the group without supplementation. All altered hematological parameters were significantly (p < 0.05) corrected by the STL supplementation in the TDNPs-exposed fish.

TABLE 2 Effects of titanium dioxide nanoparticle (TDNPs) exposure and/or dietary α -sitosterol (STL) supplementation for 60 days on the growth performance of *Oreochromis niloticus*.

	Control	STL	TDNPs	STL + TDNPs
Initial body weight (g)	11.83 ± 0.73	12.03 ± 0.54	11.33 ± 0.88	11.97 ± 0.32
Final body weight (g)	27.00 ± 1.15 ^b	36.00 ± 1.15 ^a	20.32 ± 1.03 °	23.47 ± 0.35 bc
Weight gain (g)	15.17 ± 0.44 ^b	23.97 ± 0.65 a	8.98 ± 0.30 ^d	11.50 ± 0.40 °
Daily weight gain (g/day)	0.25 ± 0.01 ^b	0.40 ± 0.01 ^a	0.15 ± 0.01 ^d	0.19 ± 0.01 °
Specific growth rate (%)	1.38 ± 0.03 ^b	1.83 ± 0.03 ^a	0.98 ± 0.05 °	1.12 ± 0.04 °
Feed intake (g)	22.17 ± 0.44 ^b	25.00 ± 0.58 ^a	18.50 ± 0.29 °	20.00 ± 0.58 bc
Feed conversion ratio	1.46 ± 0.01 °	1.04 ± 0.01 ^d	2.06 ± 0.06 ^a	1.74 ± 0.05 ^b
Survival rate	97.78 ± 2.22 ^a	100.00 ± 0.00 ^a	80.00 ± 3.85 ^b	93.33 ± 3.85 ^a
Condition factor	2.34 ± 0.01 ^b	2.58 ± 0.03 ^a	2.02 ± 0.03 °	2.23 ± 0.04 ^b

Data are presented as mean \pm standard error (n = 5 aquariums per treatment and 15 fish per aquarium). Values with different superscript letters (a, b, c, and d) within the same row indicate statistically significant differences among groups (p < 0.05). Statistical comparisons were performed using one-way ANOVA followed by Tukey's multiple comparison test.

3.3 Impact on hepatic function parameters, lipid profile, and renal injury markers

The modifications in serum liver enzymes, lipid profiles, and kidney damage indicators in fish subjected to TDNPs and/or diets comprising STL for 60 days are shown in Table 4. Exposure to TDNPs significantly (p < 0.05) increased the levels of serum enzymes [ALT (151.36%), AST (147.62%), and ALP (48.93%)], as well as urea (62.63%) and creatinine (86.79%). The combination of STL supplementation and TDNPs exposure significantly (p < 0.05) influenced the serum levels of ALT, ALP, AST, urea, and creatinine. Incorporating STL into the diet displayed no significant alterations in the mentioned variables (p > 0.05) when compared with the group receiving a non-supplemented diet.

In terms of the lipid profile, a significant decrease (p < 0.05) was detected in total cholesterol (18.43%), triglycerides (24.87%), and LDL-C (13.65%), while HDL-C increased by 24.51% after the fish were administered STL for 60 days (Table 4). On the other hand, exposure to TDNPs significantly elevated the lipid profile compared to the other groups. Notably, the STL + TDNPs group exhibited a significant (p < 0.05) reduction in cholesterol, triglyceride, and LDL-C levels, along with an increase in HDL-C, compared to the TDNPs group. These values approached those of the control group, with differences of only 4.53%, 4.92%, 10.86%, and 10.98%, respectively.

3.4 Stress indicators

Fish in the TDNPs group exhibited notably higher levels of blood glucose (27.81%) and cortisol (57.70%) compared to fish in other groups (p < 0.05). In contrast, compared to fish-fed basal diets without supplements, the inclusion of STL supplements led to significant reductions (p < 0.05) in glucose (19.10%) and cortisol (17.42%) levels. The dietary supplementation of STL to TDNPs-exposed groups normalized the glucose and cortisol levels (Table 4).

3.5 Effects on innate immunity parameters

The effects of TDNPs and/or STL on the non-specific immunological parameters of *O. niloticus* after a 60-day exposure are presented in Figure 1. The TDNPs group displayed a significant (p < 0.05) decrease in lysozyme activity (37.58%), C3 (21.72%), NO (52.44%), phagocytic activity (48.63%), and NBT (46.67%) compared to the control group. Conversely, the STL group demonstrated significantly (p < 0.05) higher levels of lysozyme activity (56.22%), C3 (13.74%), NO (37.5%), phagocytic activity (67.95%), and NBT (73.33%) when compared to the control group. In contrast, the immunological parameters in the serum of the STL + TDNPs group were improved compared to those of the TDNPs group, with levels nearly aligning with control values (p < 0.05) at 9.77%, 6.38%, 12.5%, 9.32%, and 20%, respectively.

3.6 Effects on hepatic antioxidant variables

As represented in Figure 2, fish that were exposed to TDNPs exhibited significantly (p < 0.05) lower levels of enzymatic antioxidants [CAT (46.23%), SOD (47.60%), and GPx (35.61%)] compared to the control fish, while displaying considerably (p < 0.05) higher levels of MDA (105.43%). Notably, liver tissues from fish fed a diet enriched with STL showed significant (p < 0.05) enhancements in CAT (27.64%) and SOD (14.03%) levels when compared to fish on a non-supplemented diet. In the TDNPs-exposed group, co-supplementation with STL significantly (p < 0.05) improved the aforementioned parameters, with values closely resembling those of the control group.

3.7 Impact on mRNA expression of genes involved in ER stress

As shown in Figure 3, the mRNA expression levels of *chop* (9.15-fold), *jnk* (12.66-fold), *xbp-1* (9.31-fold), and *perk* (12.50-fold)

TABLE 3 Effects of titanium dioxide nanoparticle (TDNPs) exposure and/or dietary α -sitosterol (STL) supplementation for 60 days on hematological indices of *Oreochromis niloticus*.

	Control	STL	TDNPs	STL + TDNPs	
Erythrogram					
RBCs (10 ⁶ /μL)	2.17 ± 0.04 ^b	2.41 ± 0.04 ^a	1.19 ± 0.02 °	2.07 ± 0.04 ^b	
HB (g/dL)	9.57 ± 0.60 ^a	10.93 ± 0.12 ^a	6.36 ± 0.06 °	7.95 ± 0.09 ^b	
PCV (%)	22.67 ± 0.35 ^b	23.88 ± 0.07 ^a	16.11 ± 0.11 ^d	20.81 ± 0.17 °	
MCV (fL)	104.50 ± 1.81 ^b	99.17 ± 1.26 ^b	135.43 ± 2.64^{a}	100.57 ± 0.97 ^b	
MCH (pg)	44.03 ± 1.96 bc	45.40 ± 1.16 ^b	53.47 ± 1.16 ^a	38.40 ± 0.31 °	
MCHC (%)	42.13 ± 2.09 ^{ab}	45.77 ± 0.58 ^a	39.47 ± 0.09 ^b	38.20 ± 0.12 ^b	
Leucogram	Leucogram				
WBCs (10 ³ /μL)	4.43 ± 0.05 ^a	4.62 ± 0.04 ^a	2.80 ± 0.04 °	4.09 ± 0.07 ^b	
Heterophils (10³/μL)	1.13 ± 0.02 ^a	1.18 ± 0.01^{a}	0.76 ± 0.01 °	1.03 ± 0.02 ^b	
Lymphocytes (10 ³ /μL)	2.13 ± 0.02 ^b	2.21 ± 0.01 ^a	1.47 ± 0.01 °	2.07 ± 0.01 ^b	
Eosinophils (10³/μL)	0.31 ± 0.01 ab	0.33 ± 0.01 ^a	0.20 ± 0.01 °	0.27 ± 0.01 ^b	
Monocytes (10 ³ / μL)	0.86 ± 0.01 ^a	0.90 ± 0.01 ^a	0.37 ± 0.01 °	0.72 ± 0.02 ^b	

Data are presented as mean \pm standard error (n=15). Values with different superscript letters (a, b, and c) within the same row indicate statistically significant differences among groups (p < 0.05). Statistical comparisons were performed using one-way ANOVA followed by Tukey's multiple comparison test. RBCs, red blood cell count; Hb, hemoglobin; PCV, packed cell volume; MCV, mean corpuscular volume; MCH, mean corpuscular hemoglobin; MCHC, mean corpuscular hemoglobin concentration; WBCs, white blood cell count.

in the TDNPs group were significantly elevated compared to the control group (p < 0.05). Yet, in the STL + TDNPs group, the mRNA expression levels of *chop* (3.28-fold), *jnk* (5.66-fold), *xbp-1* (3.22-fold), and *perk* (5.03-fold) were substantially lower than those in the TDNPs group (p < 0.05). When comparing the control and STL groups, no statistically significant change was found (p > 0.05).

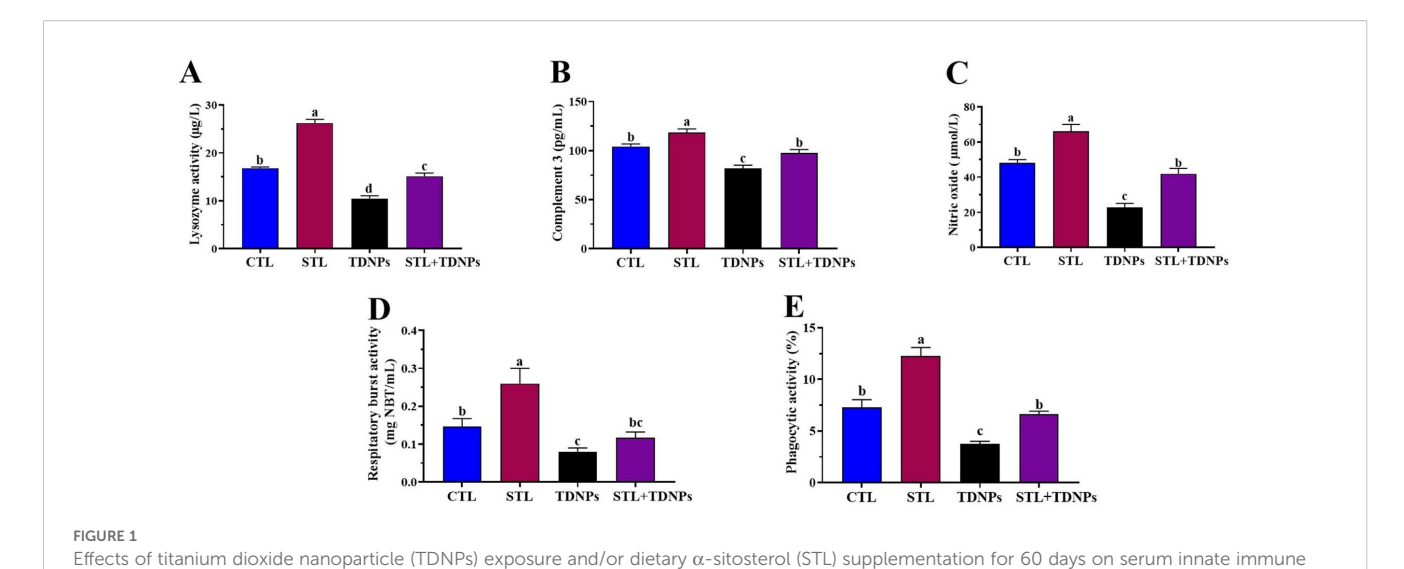
3.8 Impact on mRNA expression of genes involved in autophagy

As displayed in Figure 4, there were no significant variations (p > 0.05) in the expression levels of *beclin-1*, *mtor*, *lc3-ii*, and *p62* when comparing the STL group to the control group (p > 0.05). In the group

TABLE 4 Effects of titanium dioxide nanoparticle (TDNPs) exposure and/or dietary α -sitosterol (STL) supplementation for 60 days on some serum biochemical indices of *Oreochromis niloticus*.

	Control	STL	TDNPs	STL + TDNPs
ALT (U/L)	25.33 ± 1.20 b	23.00 ± 1.15 ^b	63.67 ± 4.67 ^a	34.00 ± 2.08 ^b
AST (U/L)	29.67 ± 0.88 ^b	25.33 ± 2.03 ^b	73.47 ± 4.28 ^a	31.17 ± 0.73 ^b
ALP (U/L)	36.93 ± 1.10 ^b	35.37 ± 0.84 ^b	55.00 ± 2.89 ^a	40.00 ± 1.15 ^b
Urea (mg/dL)	2.81 ± 0.06 ^b	2.81 ± 0.09 b	4.57 ± 0.23 ^a	3.05 ± 0.08 ^b
Creatinine (mg/dL)	0.53 ± 0.02 bc	0.46 ± 0.02 °	0.99 ± 0.01 ^a	0.61 ± 0.02 b
TC (mg/dL)	110.33 ± 1.45 ^b	90.00 ± 1.15 °	127.33 ± 1.45 ^a	115.33 ± 1.45 ^b
TG (mg/dL)	92.77 ± 1.25 ^b	69.70 ± 1.42 °	107.33 ± 1.45 ^a	97.33 ± 0.88 ^b
HDL-C (mg/dL)	26.77 ± 0.72 b	33.33 ± 0.88 ^a	20.17 ± 0.60 °	23.83 ± 1.01 bc
LDL-C (mg/dL)	75.77 ± 1.97 °	65.43 ± 1.44 ^d	93.83 ± 1.64 ^a	84.00 ± 2.08 ^b
Glucose (mg/dL)	74.33 ± 2.33 ^b	60.13 ± 0.59 °	95.00 ± 2.65 ^a	81.00 ± 2.08 ^b
Cortisol (ng/mL)	56.10 ± 1. 24 ^b	46.33 ± 1.45 °	88.47 ± 1.35 ^a	60.67 ± 0.88 ^b

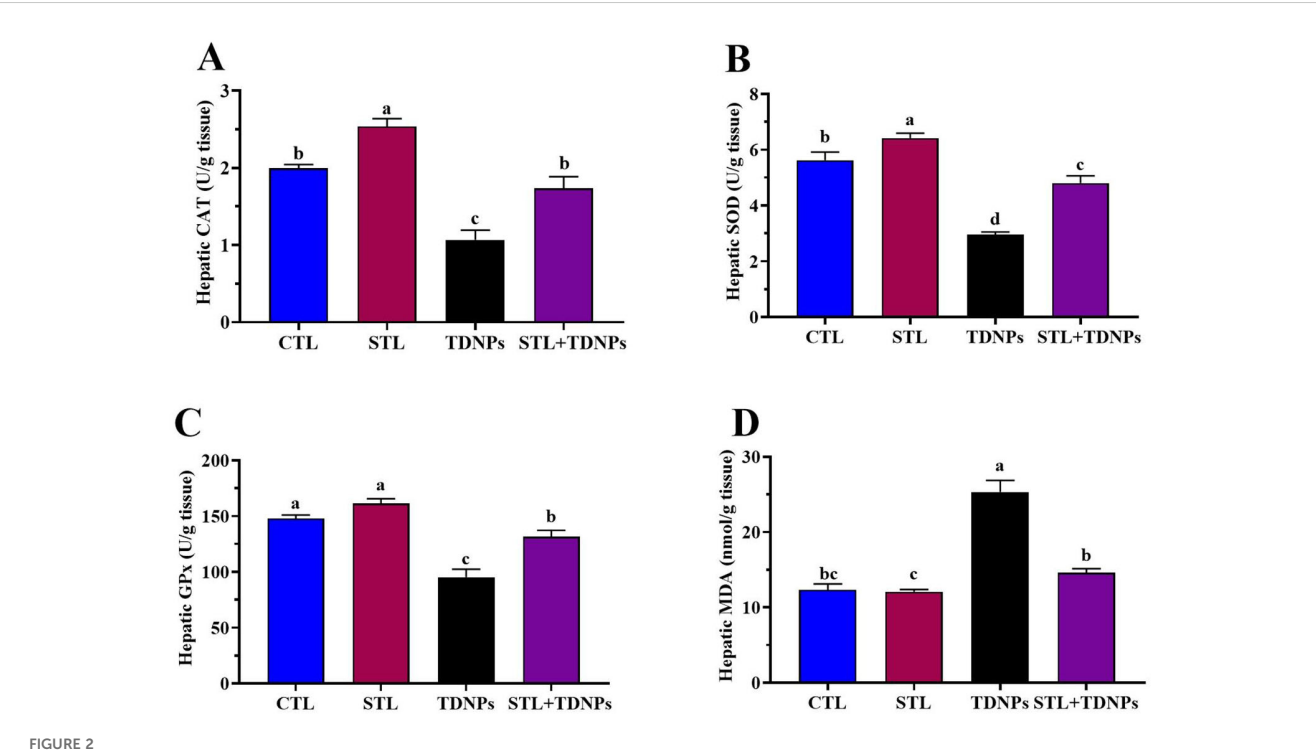
Data are presented as mean \pm standard error (n=15). Values with different superscript letters (a, b, and c) within the same row indicate statistically significant differences among groups (p < 0.05). Statistical comparisons were performed using one-way ANOVA followed by Tukey's multiple comparison test. ALT, alanine aminotransferase; AST, aspartate aminotransferase; ALP, alkaline phosphatase; TC, total cholesterol; TG, triglycerides; HDL-C, high-density lipoprotein cholesterol; LDL-C, low-density lipoprotein cholesterol.



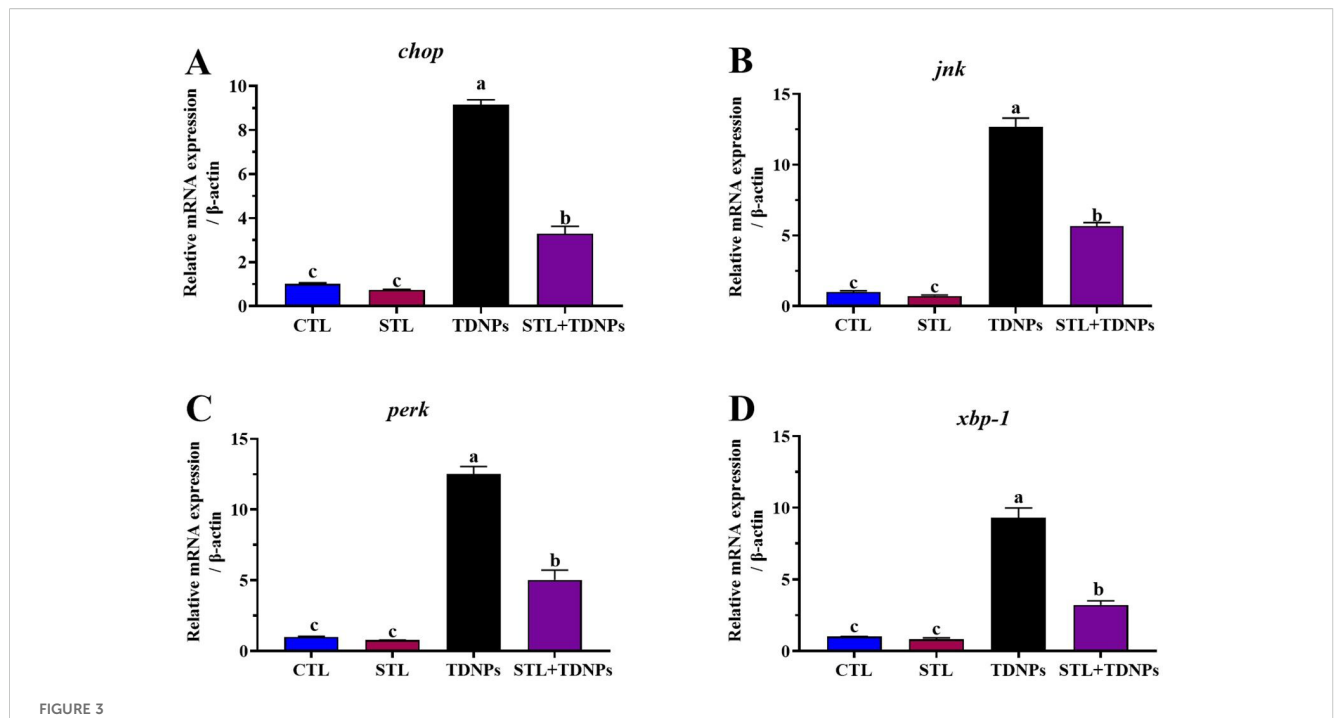
parameters in *Oreochromis niloticus*: (A) lysozyme activity, (B) complement 3 (C3) content, (C) nitric oxide (NO) concentration, (D) respiratory burst activity, and (E) phagocytic activity (%). Data are presented as mean \pm standard error (n = 15). Statistical comparisons were performed using one-way ANOVA followed by Tukey's multiple comparison test. Bars with different superscript letters (a, b, and c) indicate statistically significant differences among groups (p < 0.05).

exposed to TDNPs, a significant increase (p < 0.05) in mtor (7.15-fold) and p62 (10.57-fold) gene expression and a significant decrease (p < 0.05) in beclin-1 (0.21-fold) and lc3-ii (0.28-fold) gene expression were observed when compared to the control group. Conversely, the group

treated with both STL and TDNPs exhibited notable downregulation of mtor~(3.01-fold) and p62~(3.15-fold) genes, along with significant upregulation (p<0.05) in beclin-1~(0.67-fold) and lc3-ii~(0.90-fold) gene expression in comparison to the group exposed to TDNPs.



Effects of titanium dioxide nanoparticle (TDNPs) exposure and/or dietary α -sitosterol (STL) supplementation for 60 days on hepatic oxidative stress biomarkers in *Oreochromis niloticus*: **(A)** catalase (CAT) activity, **(B)** superoxide dismutase (SOD) activity, **(C)** glutathione peroxidase (GPx) content, and **(D)** malondialdehyde (MDA) concentration. Data are presented as mean \pm standard error (n=15). Statistical comparisons were performed using one-way ANOVA followed by Tukey's multiple comparison test. Bars with different superscript letters (a, b, c, and d) indicate statistically significant differences among groups (p < 0.05).



Effects of titanium dioxide nanoparticle (TDNPs) exposure and/or dietary α -sitosterol (STL) supplementation for 60 days on hepatic mRNA expression of ER stress-related genes in *Oreochromis niloticus*: (A) C/EBP homologous protein (*chop*), (B) c-Jun N-terminal kinase (*jnk*), (C) protein kinase RNA-like endoplasmic reticulum kinase (*perk*), and (D) X-box binding protein 1 (*xbp-1*). Data are presented as mean \pm standard error (n=15). Statistical comparisons were performed using one-way ANOVA followed by Tukey's multiple comparison test. Bars with different superscript letters (a, b, and c) indicate statistically significant differences among groups (p < 0.05).

3.9 Histopathological investigations

Histological examinations revealed organ-specific pathological alterations following TDNPs exposure, with varying degrees of severity across the intestine, liver, kidney, and spleen. Representative photomicrographs for all organs are presented in Figures 5–8, while corresponding lesion scores are detailed in Table 5. Notably, STL dietary supplementation demonstrated a consistent protective effect across all examined tissues, reducing the extent and severity of TDNPs-induced damage.

3.9.1 Intestine

Histological sections of intestines from the control (Figure 5A) and STL-supplemented groups (Figure 5B) showed normal architecture, including intact mucosal villi, submucosa, musculosa, and serosa. The STL group exhibited more elongated and branched villi. In contrast, the intestines of the TDNPs-exposed group (Figure 5C) demonstrated severe pathological alterations, including significant desquamation of mucosal epithelium (3.20 \pm 0.20), submucosal edema (1.80 \pm 0.25), and leukocytic infiltration (2.70 \pm 0.30), all of which were significantly higher (p < 0.05) compared to control and STL groups. Co-treatment with STL (Figure 5D) ameliorated these effects, as indicated by significantly reduced lesion scores for mucosal desquamation (0.90 \pm 0.28) and submucosal edema (0.50 \pm 0.17).

3.9.2 Liver

Liver tissues from control (Figure 6A) and STL groups (Figure 6B) maintained normal histo-morphological configurations,

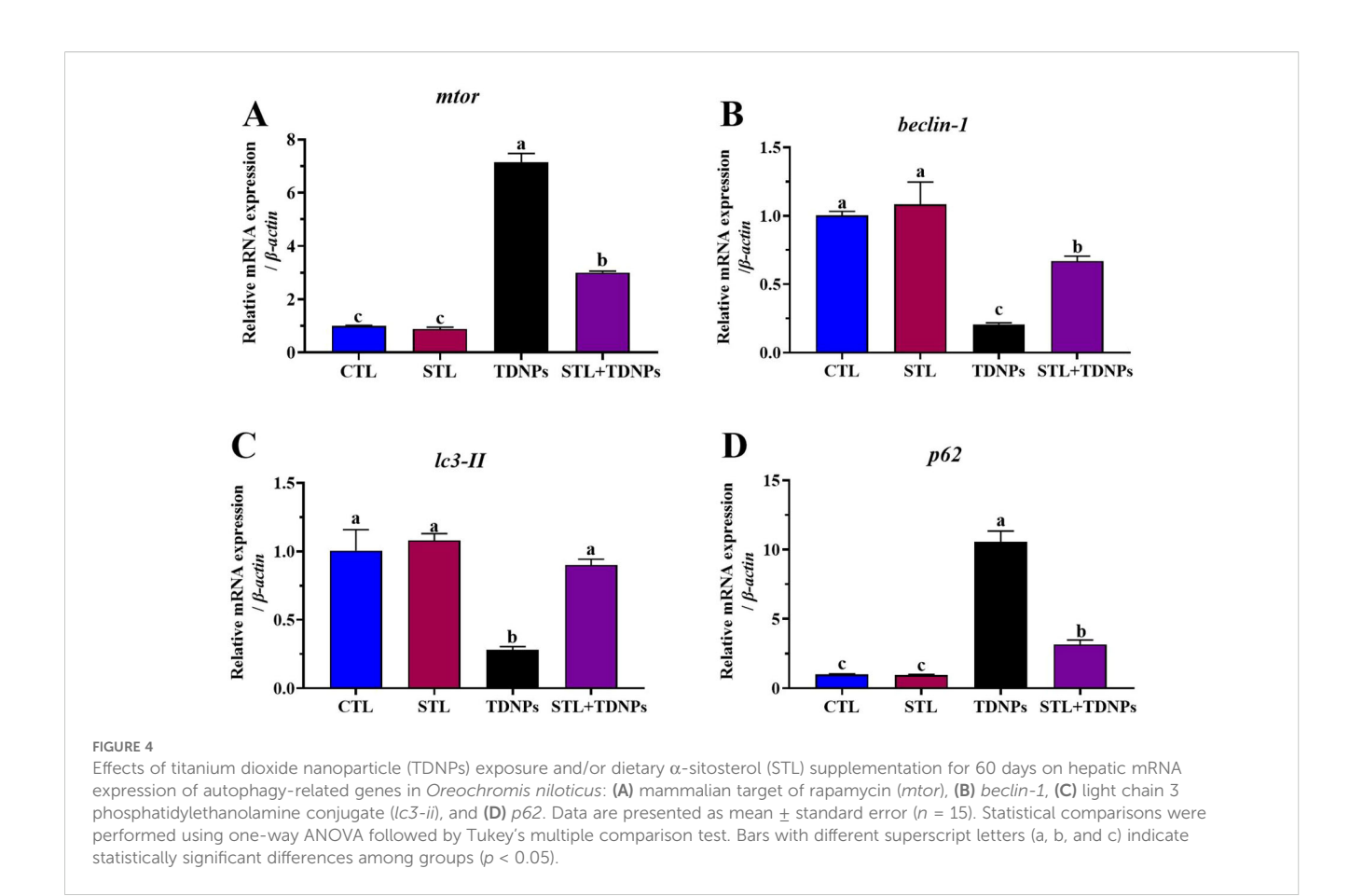
including pancreatic acini and hepatocytes. However, TDNPs exposure (Figure 6C) caused significant (p < 0.05) hepatic degeneration, characterized by necrotic hepatocytes (2.20 \pm 0.25), degenerated hepatocytes (2.90 \pm 0.23), perivascular inflammatory infiltrates (2.60 \pm 0.31), and congestion of blood vessels (2.70 \pm 0.30), all significantly elevated versus control. STL co-treatment (Figure 6D) led to marked improvement, with significantly (p < 0.05) lower scores for hepatocellular degeneration (0.70 \pm 0.26), necrosis (0.30 \pm 0.15), and inflammatory infiltrates (0.70 \pm 0.21).

3.9.3 Kidney

Renal tissues from control (Figure 7A) and STL groups (Figure 7B) showed preserved glomeruli and tubules. Conversely, the TDNPs group (Figure 7C) exhibited severe renal damage, including necrotic tubular epithelium (2.90 \pm 0.23), hypocellular glomeruli (1.80 \pm 0.25), and vascular congestion (2.90 \pm 0.23), all significantly (p < 0.05) increased compared to controls. STL supplementation (Figure 7D) attenuated renal injury, as evidenced by reduced lesion scores for necrotic tubules (0.40 \pm 0.16), glomerular damage (0.70 \pm 0.21), and congestion (0.70 \pm 0.21), with statistically significant (p < 0.05) improvement over the TDNPs group.

3.9.4 Spleen

Spleen sections from control (Figure 8A) and STL groups (Figure 8B) had normal cytoarchitecture with intact white pulp and melanomacrophage centers. The TDNPs group (Figure 8C) displayed prominent splenic alterations, including depleted white



pulp (2.20 \pm 0.20), increased melanomacrophage centers (2.80 \pm 0.25), and pelosis (2.90 \pm 0.28), which were significantly (p < 0.05) higher than in controls. The STL + TDNPs group (Figure 8D) displayed significant (p< 0.05) restoration in splenic architecture, with white pulp depletion reduced to 0.50 \pm 0.17 and melanomacrophage score lowered to 1.90 \pm 0.18.

Lesion scores summarized in Table 5 underscore the differential susceptibility of each organ to TDNPs-induced toxicity. Among the tissues examined, the liver and kidney exhibited the highest lesion severity, followed by the spleen and intestine. STL supplementation significantly attenuated pathological changes in all organs, with the most notable protective effects observed in renal and hepatic tissues.

4 Discussion

In the current study, dietary STL markedly ameliorated the multiple adverse effects induced by 60-day waterborne exposure to 10 mg/L TDNPs in Nile tilapia. TDNPs alone caused growth suppression, hematological disruption, immunosuppression, oxidative stress, ER stress, and autophagy dysregulation. In contrast, STL co-treatment restored these parameters toward control levels, likely via improved intestinal integrity, enhanced antioxidant defenses, and modulation of stress- and autophagy-related gene expression.

4.1 Growth performance and intestinal morphology

Herein, fish exposed to 10 mg/L TDNPs for 60 days exhibited a significant reduction in growth performance indicators compared with controls, consistent with growth retardation reported in carp under similar TDNPs exposures (e.g., 1 mg/L TDNPs for 10 days; Haghighat et al., 2021). The observed villus atrophy and epithelial desquamation in the anterior intestine of TDNPs-exposed fish point to impairment of nutrient absorption due to oxidative and inflammatory injury to the intestinal mucosa, reducing digestive enzyme activity and nutrient uptake, thereby reducing growth (Cunha and De Brito-Gitirana, 2020; MaChado Kayser et al., 2022). In contrast, STL supplementation (80 mg/kg diet) preserved villus height and mucosal integrity, and improved FI, feed efficiency, and growth performance. Mechanistically, STL's antioxidant properties limit ROS-induced lipid peroxidation in enterocytes, while its membrane-stabilizing and antiinflammatory effects maintain barrier function and nutrient transport capacity (El-Houseiny et al., 2025). Additionally, improved activities of intestinal digestive enzymes, particularly protease activity under STL, have been reported in largemouth bass (Micropterus salmoides) receiving phytosterol-enriched diets (0.1% and 0.5%) for 56 days, which could consequently enhance feed utilization efficiency (Liang et al., 2024).

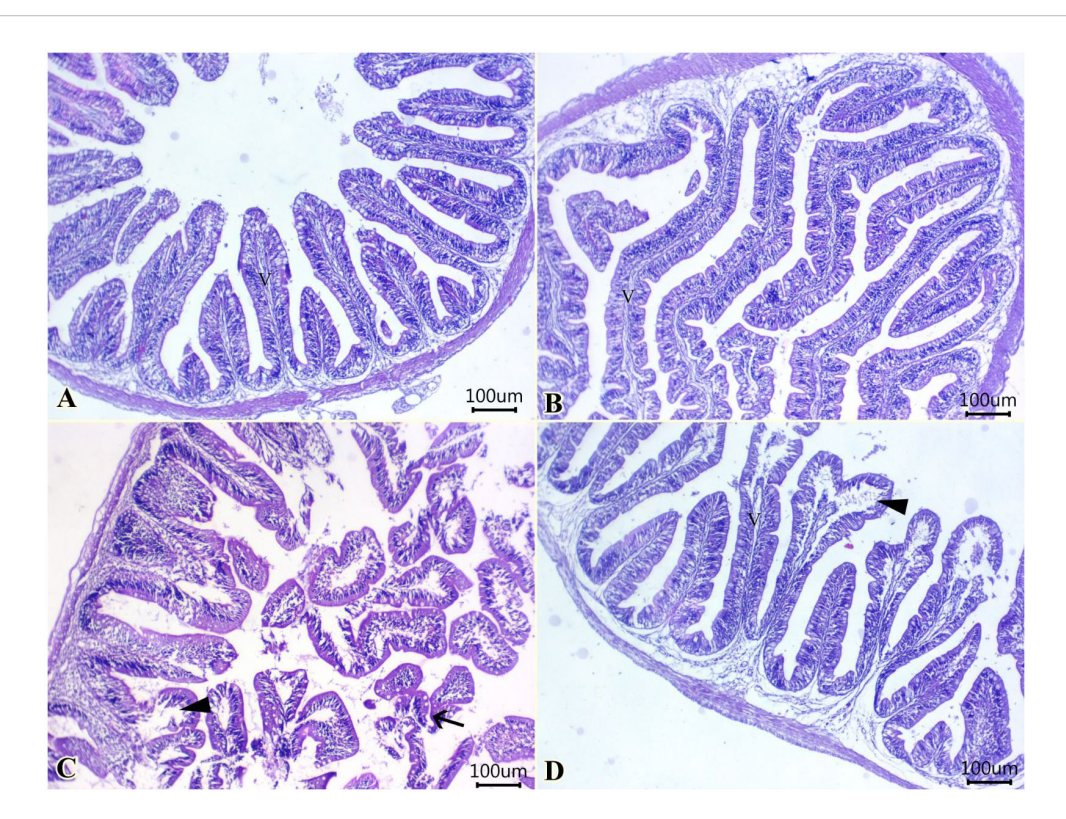


FIGURE 5 (A–D) Representative photomicrographs of H&E-stained sections from the intestine showing normal mucosal villi (V), submucosa, musculosa, and serosa in both control (A) and α -sitosterol (STL)-treated fish (B). Desquamated sheets of mucosal epithelium (arrow), and edema within lamina propria, submucosa (arrowhead) in titanium dioxide nanoparticle (TDNPs)-exposed fish (C). Mild edema within the submucosal layer (arrowhead) at the STL + TDNPs group (D) with apparently normal villi, and the muscular layer. H&E bar, 100 μ m.

4.2 Hematological parameters

TDNPs exposure macrocytic normochromic anemia, evidenced by decreased RBC, Hb, and PCV and increased MCV and MCH, which is probably mediated by erythrocyte oxidative injury, hemolysis, and membrane lipid oxidation (Vasantharaja et al., 2015). Specifically, TDNPs exposure in *T. carolinus* (3.0 µg/g by I/P injection) provoked the formation of various erythrocyte nuclear aberrations and micronuclei and subsequently diminished erythrocyte viability (Vignardi et al., 2015). Additionally, the electrostatic interactions between TDNPs surfaces and negatively charged erythrocyte membrane lipids could cause structural perturbations, leading to echinocyte formation and leakage of Hb (Li et al., 2008). Leukopenia and reduced differential counts further confirm TDNPs interference with hematopoietic tissues, possibly through direct ROS damage to spleen and kidney progenitor cells (Carmo et al., 2019).

Instead, STL co-treatment restored RBC, Hb, PCV, and WBC counts, likely through reinforcement of antioxidant defense systems (CAT, SOD, and GPx) that protect hematopoietic niches from ROS-induced damage, reflected in the enhanced splenic architecture (El-Houseiny et al., 2025). STL may also enhance hepatic erythropoietic support via upregulation of antioxidant gene expression and improved protein synthesis capacity (Ji et al., 2021). These mechanistic effects collectively indicate that STL acts as both an antioxidant and a cytoprotective modulator of erythropoiesis under NPs stress.

4.3 Hepatic and renal function biomarkers

Exposure to TDNPs significantly increased serum ALT, AST, and ALP levels and elevated urea and creatinine, indicating hepatic enzyme leakage and renal dysfunction due to oxidative and inflammatory tissue damage (Banaee et al., 2019). Histopathological findings of hepatic necrosis and renal tubular degeneration confirm this hepatonephrotoxicity. In contrast, STL co-administration lowered these enzymes and renal indices, indicating hepatoprotective and nephroprotective actions. Comparable hepatoprotective effects of dietary STL (60 and 80 mg/kg diet for 60 days) were recently reported in Nile tilapia by El-Houseiny et al. (2025). STL's hepatoprotective and nephroprotective mechanisms likely involve attenuation of oxidative stress via radical scavenging, stabilization of cellular membranes, and upregulation of endogenous antioxidant systems (Gumede et al., 2024). STL has been shown to modulate lipid metabolism, suppress inflammatory cytokine expression, and promote hepatocellular regeneration (Devaraj et al., 2020). These combined effects support restoration of hepatic enzyme activities and renal function, reducing serum urea and creatinine accumulation.

4.4 Serum lipid profile and stress indices

Herein, the dyslipidemia observed in TDNPs-exposed fish (elevated TC, TG, and LDL-C and reduced HDL-C) reflects

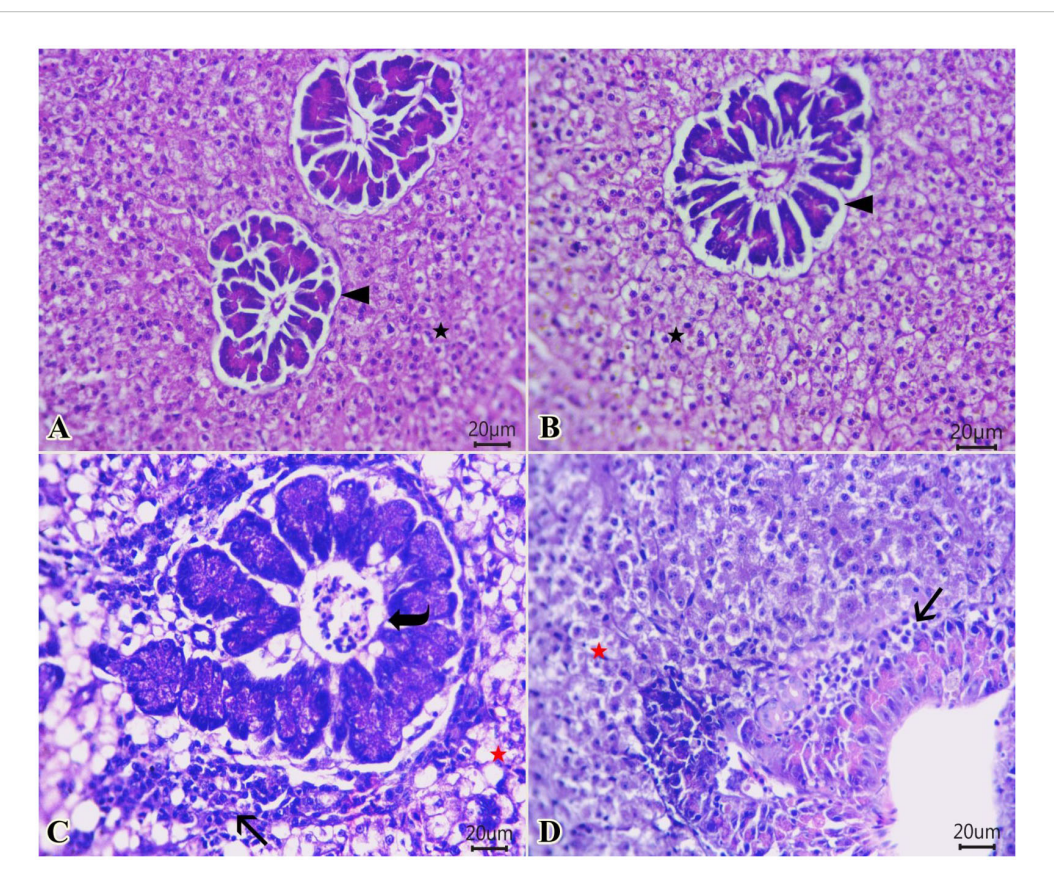


FIGURE 6

(A—D) Representative photomicrographs of H&E-stained sections from liver showing normal histo-morphological structures of hepatocytes, pancreatic acini, and vascular tissues in both control (A) and STL-treated fish (B). Diffuse areas of necrosis (red star) and hydropic degeneration within a large number of hepatocytes, peripancreatic round cell infiltrations (arrow), and congested portal veins (curved arrow) in TDNPs-exposed fish (C). Unicellular necrotic hepatocytes (red star) and a minute number of peripancreatic lymphocytes (arrow) at the STL + TDNPs group (D). H&E bar, 20 µm.

disrupted hepatic lipid metabolism and oxidative damage to lipoproteins. TDNPs can interfere with lipid homeostasis by inducing ER stress and oxidative modification of apolipoproteins (Anagha et al., 2019). Furthermore, TDNPs-exposed fish showed elevated serum glucose and cortisol levels, indicating stress-induced hyperglycemia, possibly due to activation of gluconeogenic pathways and glycogenolysis (Banaee et al., 2019; Hajirezaee et al., 2020). TDNPs-induced oxidative stress may activate the hypothalamic-pituitary-interrenal axis, increasing cortisol production and subsequently promoting gluconeogenesis, which leads to elevated glucose levels (Canli et al., 2018; Carmo et al., 2019).

In contrast, STL supplementation markedly reduced LDL-C, TC, and TG, and elevated HDL-C probably by inhibiting intestinal cholesterol absorption (competitive uptake with phytosterols) and downregulating hepatic 3-hydroxy-3-methylglutaryl-CoA reductase, while upregulating LDL receptor expression (Chen et al., 2020). In addition, phytosterols have been reported to alter cholesterol metabolism by reducing endogenous cholesterol synthesis and increasing cholesterol catabolism (Jiang et al., 2024). Moreover, STL's hypolipidemic and antioxidant properties may protect hepatocytes from steatotic injury. Furthermore, herein, STL co-treatment significantly lowered both glucose and cortisol

serum concentrations. STL mitigated these stress responses, possibly through stabilization of glucose metabolism, enhanced insulin sensitivity, and inhibition of cortisol overproduction (Ramalingam et al., 2020).

4.5 Innate immunity and phagocytic function

In this study, TDNPs exposure caused immunosuppression as evidenced by reduced lysozyme activity, C3, NO, and phagocytic activities, likely due to NPs accumulation in macrophages and interference with ROS-dependent microbial killing (Couleau et al., 2012; Hajirezaee et al., 2020). Furthermore, exposure to TDNPs has been shown to significantly alter the expression of various proinflammatory cytokines, leading to an imbalance that contributes to an inflammatory response capable of suppressing normal immune function (Vineetha et al., 2021; Sherif et al., 2022). In contrast, STL cotreatment restored innate immune responses through enhancement of macrophage phagocytic activity, increased production of lysozyme and complement factors, and stabilization of splenic and renal immune tissue architecture. STL's immunostimulatory action may derive from membrane incorporation in leukocytes, facilitating receptor-mediated

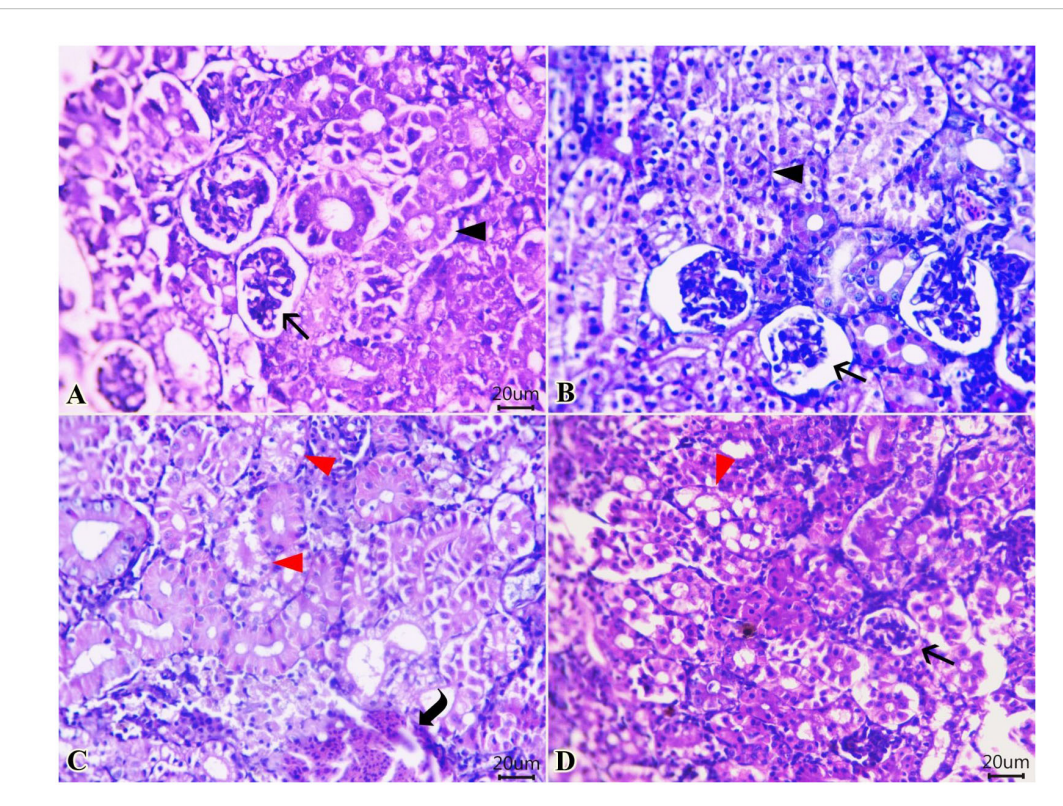


FIGURE 7

(A—D) Representative photomicrographs of H&E-stained sections from the kidney showing normal morphology of renal tubules (arrowheads), glomerular tufts (arrows), and stromal tissues in both control (A) and STL (B). Oncotic necrosis in a large number of renal tubular epithelium (red arrowheads) beside congested renal vasculature (curved arrow) in TDNPs-exposed fish (C). Improved renal parenchyma with less tubular necrosis (red arrowhead) and apparent normal glomerular tufts (arrow) at the STL + TDNPs group (D).

pathogen recognition and complement activation (Shi et al., 2013; Luhata and Usuki, 2021). Moreover, phytosterols are known to modulate immune cell signaling via the NF-κB pathway, leading to enhanced cytokine balance and immune surveillance (Song et al., 2022). In this respect, Reyes-Becerril et al. (2022) reported that a phytosterol-rich plant extract, such as the aqueous root extract of Cylindropuntia cholla, exhibited a significant immunomodulatory activity in primary cultures of tilapia peripheral blood leukocytes, as evidenced by increased phagocytic activity, respiratory burst, and NO production. Similarly, STL supplementation (60 and 80 mg/kg) for 60 days in Nile tilapia led to increased immune resilience and reduced inflammation in vital organs (El-Houseiny et al., 2025). Moreover, dietary \(\beta - STL \) (1%-2%) improved intestinal immune function by increasing lysozyme and complement levels, while augmenting antiinflammatory markers and dwindling pro-inflammatory cytokines in large yellow croaker (Larimichthys crocea) (Song et al., 2022).

4.6 Oxidative stress, autophagy, and ER stress

In the current study, TDNPs induced hepatic oxidative stress, as evidenced by decreased activities of CAT, SOD, and GPx, alongside increased MDA levels, indicating lipid peroxidation. This is consistent with previous reports showing that TDNPs generate

ROS, which damage cellular components and trigger lipid peroxidation in fish (Carmo et al., 2019; Tang et al., 2019; Bobori et al., 2020). Elevated ROS levels can further disrupt ER homeostasis, leading to the accumulation of misfolded proteins and activation of the ER stress response (Chen et al., 2021; Uribe-García et al., 2025). This response is mediated by the unfolded protein response, primarily regulated through three ER stress sensors: inositolrequiring enzyme 1α (IRE1α), PERK, and activating transcription factor 6 (ATF6) (Credle et al., 2005). Upon ER stress, these sensors are activated following dissociation from binding immunoglobulin protein (BiP), an ER chaperone involved in protein folding (Smith and Wilkinson, 2017). IRE1α promotes splicing of XBP-1 mRNA and activation of JNK, enhancing the protein-folding capacity, whereas PERK reduces global protein synthesis to alleviate ER load (Jiang et al., 2021; Shi et al., 2023). ER stress is intimately linked to autophagy, a protective mechanism that removes misfolded proteins and damaged organelles (Rashid et al., 2015). Activation of the IRE1 and PERK pathways can induce autophagy via JNK signaling and beclin-1 modulation (Shi et al., 2023). Conversely, the mTOR pathway negatively regulates autophagy by inhibiting AMPactivated protein kinase signaling (Kim et al., 2011). Herein, TDNPs exposure significantly upregulated ER stress-related genes (chop, jnk, xbp-1, and perk), while downregulating autophagy-related genes (beclin-1 and lc3-ii) and upregulating mtor and p62, indicating ER initiation and autophagy inhibition. Similarly, TDNP exposure

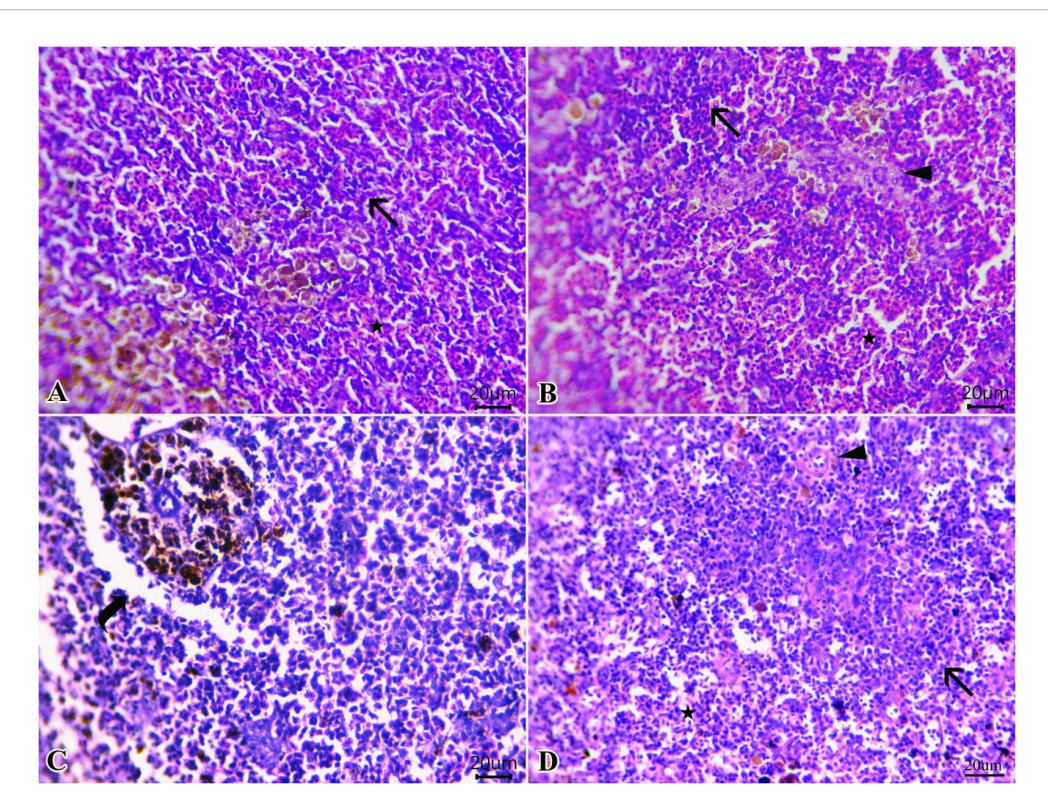


FIGURE 8

(A—D) Representative photomicrographs of H&E-stained sections from spleen showing normal histology of white pulps (arrow) around central arterioles (arrowhead) alternated with red pulps (star) in both control (A) and STL (B). Low density of lymphoid elements, particularly at the white pulp (curved arrow) in TDNPs-exposed fish (C). Re-populated cytoarchitectures of white pulp (arrow) around the ellipsoidal arterioles (arrowhead) beside normal red pulp (star) at the STL + TDNPs group (D). H&E bar, 20 µm.

has been reported to dysregulate autophagy markers, including beclin-1, lc3, and p62, ultimately leading to autophagy inhibition and cellular necrosis in zebrafish models (Kotil et al., 2017; Siqueira et al., 2021). Collectively, TDNPs initiate a cascade in which oxidative stress triggers ER stress, which, in turn, modulates autophagy pathways, culminating in hepatic cell dysfunction. On the other hand, STL co-treatment restored antioxidant enzyme activities and reduced MDA. Similarly, dietary supplementation with STL at 60 and 80 mg/kg significantly increased hepatic GPx, CAT, and SOD activities in Nile tilapia after 60 days of feeding (El-Houseiny et al., 2025). Dietary STL antioxidant capacity could be strongly related to its role as a hydrogen donor or its capability to directly counteract stable free radicals (Cheng et al., 2019). Of note, STL also normalized UPR gene expression and autophagy markers in the hepatic tissues of TDNPs-exposed fish. Recently, β-STL enhanced autophagic activity by promoting lc3-i conversion to lc3-ii and p62 degradation in lipopolysaccharide-stimulated RAW264.7 macrophages (Li et al., 2024). Similarly, in endothelial cells, β-STL suppresses inflammatory cytokine production by regulating MAPK and NFκB signaling, which is associated with autophagic activity (Bi et al., 2023). These effects likely stem from STL's free-radical scavenging and membrane-protective properties (Zhang et al., 2023), which alleviate ER stress and permit autophagic flux. Moreover, Tang et al. (2024) reported that a key mechanism through which β-STL could reduce ER stress involves the modulation of cholesterol

metabolism and the inhibition of cholesterol overload, which is a known trigger for ER stress. Moreover, Abo-Zaid et al. (2023) suggested that the antisteatotic effects of $\beta\text{-STL}$ may alleviate lipid accumulation in rats fed a high-fat diet, thereby reducing ER stress. In line with this, our study demonstrated a pronounced cholesterollowering effect of STL, with a significant reduction in LDL-C.

However, some limitations of this study should be acknowledged. The experiment was conducted under controlled laboratory conditions using a single exposure concentration (10 mg/L TDNPs) and a single dietary STL dose (80 mg/kg), which may not fully represent environmental exposure scenarios. Natural water systems contain fluctuating NPs concentrations and complex physicochemical interactions that could alter bioavailability and toxicity. Additionally, fish in natural environments are exposed to multiple stressors, including temperature variation, pathogens, and dietary differences, which may influence responses to TDNPs and STL supplementation. The present study focused on a single TDNPs concentration and dietary STL dose; thus, the dose dependency and long-term safety warrant further investigation. Future studies should incorporate doseresponse analyses to further elucidate the potential modulatory mechanisms of STL against NPs toxicity. Moreover, these findings were obtained in Nile tilapia under laboratory conditions, and their generalizability to other fish species or ecosystems remains to be validated. Investigations under semi-field or field conditions with

TABLE 5 Effects of titanium dioxide nanoparticle (TDNPs) exposure and/or dietary α -sitosterol (STL) supplementation for 60 days on lesion score of the intestinal, hepatic, renal, and splenic tissues of *Oreochromis niloticus*.

	Control	STL	TDNPs	STL + TDNPs
Intestinal tissue				
Desquamated mucosal sheets	0.00± 0.00 ^b	0.10 ± 0.10 ^b	2.70± 0.30 ^a	0.50 ± 0.17 ^b
Edema in the submucosa	$0.00 \pm 0.00^{\circ}$	0.20 ± 0.13 °	3.20 ± 0.20 ^a	0.90 ± 0.28 ^b
Leukocytic infiltrates	0.00± 0.00 b	0.10 ± 0.10 ^b	1.80 ± 0.25 ^a	0.50 ± 0.17 ^b
Hepatic tissue				
Degenerated hepatocytes	0.00 ± 0.00^{c}	0.10 ± 0.10 bc	2.90 ± 0.23 ^a	0.70 ± 0.26 ^b
Degenerated pancreatic acini	0.00 ± 0.00 ^b	0.10 ± 0.10 ^b	2.50 ± 0.29 ^a	0.60 ± 0.22 ^b
Necrotic hepatic cells	0.00 ± 0.00 ^b	0.00 ± 0.00 ^b	2.20 ± 0.25 ^a	0.30 ± 0.15 ^b
Round inflammatory cell infiltration	0.00 ± 0.00 ^b	0.20 ± 0.13 ^b	2.60 ± 0.31 ^a	0.70 ± 0.21 ^b
Congested hepatic blood vessels	$0.00^{\circ} \pm 0.00$	0.10 ± 0.10 °	2.70 ± 0.30 ^a	0.90 ± 0.18 ^b
Renal tissue				
Degenerated renal tubular epithelium	0.00 ± 0.00 °	0.10 ± 0.10 °	2.90 ± 0.23 ^a	1.00 ± 0.26 ^b
Necrotic tubular epithelium	0.00 ± 0.00 b	0.00 ± 0.00 b	2.90 ± 0.23 ^a	0.40 ± 0.16 ^b
Hypocellular glomerular tufts	0.00 ± 0.00°	0.10 ± 0.10 bc	1.80 ± 0.25 ^a	0.70 ± 0.21 ^b
Congested renal vasculatures	0.00 ± 0.00 °	0.10 ± 0.10 bc	2.90 ± 0.23 ^a	0.70 ± 0.21 ^b
Splenic tissue				
Depleted white pulp	0.00 ± 0.00^{c}	0.00 ± 0.00 °	2.20 ± 0.20 ^a	0.50 ± 0.17 ^b
Melanomacrophage centers	1.20 ± 0.13 ^c	1.20 ± 0.13 °	2.80 ± 0.25 ^a	1.90 ± 0.18 ^b
Pelosis	0.00 ± 0.00°	0.20 ± 0.13 bc	2.90 ± 0.28 ^a	0.80 ± 0.25 ^b
Interstitial edema	0.00 ± 0.00 ^b	0.00 ± 0.00 ^b	1.70 ± 0.26 ^a	0.60 ± 0.22 ^b

Data are presented as mean \pm standard error (n=15). Values with different superscript letters (a, b, and c) within the same row indicate statistically significant differences among groups (p < 0.05). Statistical comparisons were performed using the Kruskal–Wallis test followed by Dunn's post hoc test with Bonferroni correction.

varied exposure periods are therefore needed to confirm the ecological relevance and broader applicability of the present results.

5 Conclusion

This study indicated the potential of STL as an effective natural additive for mitigating the harmful effects of TDNPs in O. niloticus. The results showed that TDNPs exposure led to reduced body weight, impaired liver and kidney functions, and the onset of macrocytic normochromic anemia, leukopenia, immunosuppression, hyperlipidemia, oxidative stress, ER stress, and increased autophagy in the liver. STL effectively counteracted these adverse effects by preventing weight loss, restoring hepatic and renal functions, improving hematological and immunological parameters, and correcting lipid abnormalities. Moreover, STL reduced oxidative stress, alleviated ER stress, and modulated autophagy. These findings indicate that STL functions as a growth promoter, antioxidant, and immunostimulant, preserving tissue integrity and potentially offering health benefits relevant to human consumption. Therefore, STL may be considered a promising natural supplement for inclusion in aquafeed.

Data availability statement

The original contributions presented in the study are included in the article/Supplementary Material. Further inquiries can be directed to the corresponding authors.

Ethics statement

The animal study was approved by Animal Ethics Committee of Zagazig University's, with an approval number ZU-IACUC/2/F/85/2025. The study was conducted in accordance with the local legislation and institutional requirements.

Author contributions

AB: Writing – original draft, Data curation, Methodology, Software, Conceptualization. WE-H: Writing – original draft, Software, Conceptualization, Methodology, Data curation, Investigation. AM: Resources, Software, Writing – review & editing, Conceptualization. YA-E: Visualization, Conceptualization, Software, Writing – review &

editing. AA: Writing – review & editing, Conceptualization, Resources, Software. YA: Conceptualization, Software, Resources, Writing – review & editing. HH: Data curation, Visualization, Writing – review & editing, Software. NA-A: Methodology, Conceptualization, Writing – review & editing, Investigation.

Funding

The author(s) declare financial support was received for the research and/or publication of this article. This work was supported by the Deanship of Scientific Research, Vice Presidency for Graduate Studies and Scientific Research, King Faisal University, Saudi Arabia [Grant No. KFU254074]. Also, the authors thank all the entire staff of the Department of Aquatic Animal Medicine, Faculty of Veterinary Medicine, Zagazig University, for their support during the work.

Conflict of interest

The authors declare that the research was conducted in the absence of any commercial or financial relationships that could be construed as a potential conflict of interest.

The author(s) declared that they were an editorial board member of Frontiers, at the time of submission. This had no impact on the peer review process and the final decision.

Generative AI statement

The author(s) declare that no Generative AI was used in the creation of this manuscript.

Any alternative text (alt text) provided alongside figures in this article has been generated by Frontiers with the support of artificial intelligence and reasonable efforts have been made to ensure accuracy, including review by the authors wherever possible. If you identify any issues, please contact us.

Publisher's note

All claims expressed in this article are solely those of the authors and do not necessarily represent those of their affiliated organizations, or those of the publisher, the editors and the reviewers. Any product that may be evaluated in this article, or claim that may be made by its manufacturer, is not guaranteed or endorsed by the publisher.

Supplementary material

The Supplementary Material for this article can be found online at: https://www.frontiersin.org/articles/10.3389/fmars.2025.1700010/full#supplementary-material

References

Abdelaziz, R., Tartor, Y. H., Barakat, A. B., El-Didamony, G., Gado, M. M., Zaki, M. S. A., et al. (2024). Alpha-sitosterol: a new antiviral agent produced by *Streptomyces misakiensis* and its potential activity against Newcastle disease virus. *BMC Vet. Res.* 20, 76. doi: 10.1186/s12917-023-03875-y

Abd-Elhakim, Y. M., Hashem, M. M. M., Abo-El-Sooud, K., Mousa, M. R., Soliman, A. M., Mouneir, S. M., et al. (2023). Interactive effects of cadmium and titanium dioxide nanoparticles on hepatic tissue in rats: Ameliorative role of coenzyme 10 via modulation of the NF-kB and TNF α pathway. Food Chem. Toxicol. 182, 114191. doi: 10.1016/j.fct.2023.114191

Abdel-Khalek, A. A., Kadry, M., Badran, S. R., and Marie, M.-a. (2015). Comparative toxicity of copper oxide bulk and nano particles in Nile Tilapia; Oreochromis niloticus: Biochemical and oxidative stress. *J. Basic Appl. Zoology* 72, 43–57. doi: 10.1016/j.jobaz.2015.04.001

Abdel-Latif, H. M., Dawood, M. A., Menanteau-Ledouble, S., and El-Matbouli, M. (2020). Environmental transformation of n-TiO2 in the aquatic systems and their ecotoxicity in bivalve mollusks: A systematic review. *Ecotoxicol. Environ. Saf.* 200, 110776. doi: 10.1016/j.ecoenv.2020.110776

Abdel-Moneim, A.-M., Sabic, E., Abu-Taleb, A., and Ibrahim, N. S. (2020). Growth performance, hemato-biochemical indices, thyroid activity, antioxidant status, and immune response of growing Japanese quail fed diet with full-fat canola seeds. *Trop. Anim. Health Prod.* 52, 1853–1862. doi: 10.1007/s11250-020-02200-1

Abo-Zaid, O. A., Moawed, F. S., Ismail, E. S., and Farrag, M. A. (2023). β -sitosterol attenuates high-fat diet-induced hepatic steatosis in rats by modulating lipid metabolism, inflammation and ER stress pathway. *BMC Pharmacol. Toxicol.* 24, 31. doi: 10.1186/s40360-023-00671-0

Aebi, H. (1984). "[13] Catalase in vitro," in Methods in Enzymology (San Diego, CA, USA: Academic Press), 121–126.

Alam, M. W., Junaid, P. M., Gulzar, Y., Abebe, B., Awad, M., and Quazi, S. A. (2024). Advancing agriculture with functional NM: "pathways to sustainable and smart farming technologies. *Discov. Nano* 19, 197. doi: 10.1186/s11671-024-04144-z

Alexpandi, R., Gopi, C. V. M., Durgadevi, R., Kim, H.-J., Pandian, S. K., and Ravi, A. V. (2020). Metal sensing-carbon dots loaded TiO2-nanocomposite for photocatalytic bacterial deactivation and application in aquaculture. *Sci. Rep.* 10, 12883. doi: 10.1038/s41598-020-69888-x

Allain, C. C., Poon, L. S., Chan, C. S., Richmond, W., and Fu, P. C. (1974). Enzymatic determination of total serum cholesterol. *Clin. Chem.* 20, 470–475. doi: 10.1093/clinchem/20.4.470

Alliance, G. S. (2023). Annual farmed finfish production survey: A modest supply decline for 2023 and a predicted return to growth in 2024. Available online at: https://www.globalseafood.org/advocate/annual-farmed-finfish-production-survey-a-modest-supply-decline-for-2023-and-a-predicted-return-to-growth-in-2024/ (Accessed October 9, 2023).

Ameen, F., Alsamhary, K., Alabdullatif, J. A., and Alnadhari, S. (2021). A review on metal-based nanoparticles and their toxicity to beneficial soil bacteria and fungi. *Ecotoxicology Environ. Saf.* 213, 112027. doi: 10.1016/j.ecoenv.2021.112027

Anagha, T., Gupta, S., Srivastava, P. P., Prasad, N., Sahu, R. K., Varghese, T., et al. (2019). Antioxidant response and serum lipid changes of *Labeo rohita* exposed to intraperitoneal titanium dioxide nanoparticles. *J. Entomol. Zool. Stud.* 7, 482–487.

AOAC (2006). Official methods of analysis. 18th edn (USA, Washington, DC: AOAC International, Gaithersburg, MD).

Assmann, G., Jabs, H. U., Kohnert, U., Nolte, W., and Schriewer, H. (1984). LDL-cholesterol determination in blood serum following precipitation of LDL with polyvinylsulfate. *Clin. Chim. Acta* 140, 77–83. doi: 10.1016/0009-8981(84)90153-0

Atanda, S. A., Shaibu, R. O., and Agunbiade, F. O. (2025). Nanoparticles in agriculture: balancing food security and environmental sustainability. *Discover Agric.* 3, 26. doi: 10.1007/s44279-025-00159-x

Bain, B. J., Bates, I., Laffan, M. A., and Lewis, S. M. (2016). *Dacie and Lewis practical haematology: expert consult: online and print.* (Philadelphia, PA, USA: Elsevier Health Sciences).

Banaee, M., Tahery, S., Haghi, B., Shahafve, S., and Vaziriyan, M. (2019). Blood biochemical changes in common carp (*Cyprinus carpio*) upon co-exposure to titanium dioxide nanoparticles and paraquat. *Iran. J. Fish. Sci.* 18, 242–255. doi: 10.22092/iifs.2019.118174

Bernet, D., Schmidt, H., Meier, W., Burkhardt-Holm, P., and Wahli, T. (1999). Histopathology in fish: Proposal for a protocol to assess aquatic pollution. *J. Fish Dis.* 22, 25–34. doi: 10.1046/j.1365-2761.1999.00134.x

Bi, Y., Liang, H., Han, X., Li, K., Zhang, W., Lai, Y., et al. (2023). β -sitosterol suppresses LPS-induced cytokine production in human umbilical vein endothelial cells

- via MAPKs and NF-KB signaling pathway. Evidence-Based Complementary Altern. Med. 2023, 9241090. doi: 10.1155/2023/9241090
- Bobori, D., Dimitriadi, A., Karasiali, S., Tsoumaki-Tsouroufli, P., Mastora, M., Kastrinaki, G., et al. (2020). Common mechanisms activated in the tissues of aquatic and terrestrial animal models after TiO2 nanoparticles exposure. *Environ. Int.* 138, 105611. doi: 10.1016/j.envint.2020.105611
- Boyd, C. E., and Tucker, C. S. (2012). *Pond aquaculture water quality management.* (New York, NY, USA: Springer Science & Business Media).
- Bryan, N. S., and Grisham, M. B. (2007). Methods to detect nitric oxide and its metabolites in biological samples. *Free Radic. Biol. Med.* 43, 645–657. doi: 10.1016/j.freeradbiomed.2007.04.026
- Canli, E. G., Dogan, A., and Canli, M. (2018). Serum biomarker levels alter following nanoparticle (Al(2)O(3), CuO, TiO(2)) exposures in freshwater fish (*Oreochromis niloticus*). Environ. Toxicol. Pharmacol. 62, 181–187. doi: 10.1016/j.etap.2018.07.009
- Carmo, T. L. L., Siqueira, P. R., Azevedo, V. C., Tavares, D., Pesenti, E. C., Cestari, M. M., et al. (2019). Overview of the toxic effects of titanium dioxide nanoparticles in blood, liver, muscles, and brain of a Neotropical detritivorous fish. *Environ. Toxicol.* 34, 457–468. doi: 10.1002/tox.22699
- Chen, L., Nie, P., Yao, L., Tang, Y., Hong, W., Liu, W., et al. (2021). TiO₂NPs induce the reproductive toxicity in mice with gestational diabetes mellitus through the effects on the endoplasmic reticulum stress signaling pathway. *Ecotoxicol. Environ. Saf.* 226, 112814. doi: 10.1016/j.ecoenv.2021.112814
- Chen, S., Wang, R., Cheng, M., Wei, G., Du, Y., Fan, Y., et al. (2020). Serum cholesterol-lowering activity of β -sitosterol laurate is attributed to the reduction of both cholesterol absorption and bile acids reabsorption in hamsters. *J. Agric. Food Chem.* 68, 10003–10014. doi: 10.1021/acs.jafc.0c04386
- Cheng, Y., Chen, Y., Li, J., Qu, H., Zhao, Y., Wen, C., et al. (2019). Dietary β -sitosterol improves growth performance, meat quality, antioxidant status, and mitochondrial biogenesis of breast muscle in broilers. *Animals* 9, 71. doi: 10.3390/ani9030071
- Costas, B., Couto, A., Azeredo, R., MaChado, M., Krogdahl, Å., and Oliva-Teles, A. (2014). Gilthead seabream (*Sparus aurata*) immune responses are modulated after feeding with purified antinutrients. *Fish Shellfish Immunol.* 41, 70–79. doi: 10.1016/j.fsi.2014.05.032
- Couleau, N., Techer, D., Pagnout, C., Jomini, S., Foucaud, L., Laval-Gilly, P., et al. (2012). Hemocyte responses of *Dreissena polymorpha* following a short-term *in vivo* exposure to titanium dioxide nanoparticles: Preliminary investigations. *Sci. Total Environ.* 438, 490–497. doi: 10.1016/j.scitotenv.2012.08.095
- Credle, J. J., Finer-Moore, J. S., Papa, F. R., Stroud, R. M., and Walter, P. (2005). On the mechanism of sensing unfolded protein in the endoplasmic reticulum. *Proc. Natl. Acad. Sci. U.S.A.* 102, 18773–18784. doi: 10.1073/pnas.0509487102
- Cunha, R., and De Brito-Gitirana, L. (2020). Effects of titanium dioxide nanoparticles on the intestine, liver, and kidney of *Danio rerio. Ecotoxicol. Environ. Saf.* 203, 111032. doi: 10.1016/j.ecoenv.2020.111032
- Dawood, M., Zommara, M., Eweedah, N. M., and Helal, A. I. (2020). The evaluation of growth performance, blood health, oxidative status and immune-related gene expression in Nile tilapia (Oreochromis niloticus) fed dietary nanoselenium spheres produced by lactic acid bacteria. *Aquaculture* 515, 734571. doi: 10.1016/j.aquaculture.2019.734571
- De Silva, W., and Pathiratne, A. (2023). Nano-titanium dioxide induced genotoxicity and histological lesions in a tropical fish model, Nile tilapia (*Oreochromis niloticus*). *Environ. Toxicol. Pharmacol.* 98, 104043. doi: 10.1016/j.etap.2022.104043
- Devaraj, E., Roy, A., Royapuram Veeraragavan, G., Magesh, A., Varikalam Sleeba, A., Arivarasu, L., et al. (2020). β -Sitosterol attenuates carbon tetrachloride-induced oxidative stress and chronic liver injury in rats. *Naunyn. Schmiedebergs Arch. Pharmacol.* 393, 1067–1075. doi: 10.1007/s00210-020-01810-8
- Ding, X. Q., Yuan, C. C., Huang, Y. B., Jiang, L., and Qian, L. C. (2021). Effects of phytosterol supplementation on growth performance, serum lipid, proinflammatory cytokines, intestinal morphology, and meat quality of white feather broilers. *Poult. Sci.* 100, 101096. doi: 10.1016/j.psj.2021.101096
- Do, T. C. M. V., Nguyen, D. Q., Nguyen, K. T., and Le, P. H. (2019). TiO2 and Au-TiO2 nanomaterials for rapid photocatalytic degradation of antibiotic residues in aquaculture wastewater. *Materials* 12, 2434. doi: 10.3390/ma12152434
- El-Houseiny, W., Abdelaziz, R., Mansour, A. T., Alqhtani, H. A., Bin-Jumah, M. N., Bayoumi, Y., et al. (2025). Effects of α-sitosterol on growth, hematobiochemical profiles, immune-antioxidant resilience, histopathological features and expression of immune apoptotic genes of Nile tilapia, *Oreochromis niloticus*, challenged with *Candida albicans. Comp. Biochem. Physiol. B: Biochem. Mol. Biol.* 275, 111035. doi: 10.1016/j.cbpb.2024.111035
- Ellis, A. E. (1999). Immunity to bacteria in fish. Fish Shellfish Immunol. 9, 291–308. doi: $10.1006/\mathrm{fsim}.1998.0192$
- El-Naby, A. S. A., El Asely, A. M., Hussein, M. N., Khattaby, A.E.-R.A., and Abo-Al-Ela, H. G. (2025). Impact of dietary Biocide clay on growth, physiological status, and histological indicators of the liver and digestive tract in Nile tilapia (Oreochromis niloticus). *Sci. Rep.* 15, 5311. doi: 10.1038/s41598-025-89042-9
- El-Sayed, A.-F. M. (2021). The success story of aquacultu re in Egypt: the real motivation for hosting the first aquaculture Africa conference (AFRAQ2i). 3, 16-16.
- Fan, Y., Shen, J., Liu, X., Cui, J., Liu, J., Peng, D., et al. (2023). β-sitosterol suppresses lipopolysaccharide-induced inflammation and lipogenesis disorder in bovine mammary epithelial cells. *Int. J. Mol. Sci.* 24, 14644. doi: 10.3390/ijms241914644

- FAO (2022). "The State of World Fisheries and Aquaculture 2022," in *Towards Blue Transformation. The State of World Fisheries and Aquaculture (SOFIA)* (FAO, Rome, Italy), 266.
- Feng, S., Belwal, T., Li, L., Limwachiranon, J., Liu, X., and Luo, Z. (2020). Phytosterols and their derivatives: Potential health-promoting uses against lipid metabolism and associated diseases, mechanism, and safety issues. *Compr. Rev. Food Sci. Food Saf.* 19, 1243–1267. doi: 10.1111/1541-4337.12560
- Fossati, P., and Prencipe, L. (1982). Serum triglycerides determined colorimetrically with an enzyme that produces hydrogen peroxide. *Clin. Chem.* 28, 2077–2080. doi: 10.1093/clinchem/28.10.2077
- Fossati, P., Prencipe, L., and Berti, G. (1983). Enzymic creatinine assay: a new colorimetric method based on hydrogen peroxide measurement. *Clin. Chem.* 29, 1494–1496. doi: 10.1093/clinchem/29.8.1494
- Geletu, T. T., and Zhao, J. (2023). Genetic resources of Nile tilapia (Oreochromis niloticus Linnaeus 1758) in its native range and aquaculture. *Hydrobiologia* 850, 2425–2445. doi: 10.1007/s10750-022-04989-4
- Gumede, N. M., Lembede, B. W., Nkomozepi, P., Brooksbank, R. L., Erlwanger, K. H., and Chivandi, E. (2024). Protective effect of β -sitosterol against high-fructose dietinduced oxidative stress, and hepatorenal derangements in growing female sprague-dawley rats. *Lab. Anim. Res.* 40, 30. doi: 10.1186/s42826-024-00215-5
- Haghighat, F., Kim, Y., Sourinejad, I., Yu, I. J., and Johari, S. A. (2021). Titanium dioxide nanoparticles affect the toxicity of silver nanoparticles in common carp (Cyprinus carpio). *Chemosphere* 262, 127805. doi: 10.1016/j.chemosphere. 2020.127805
- Hajirezaee, S., Mohammadi, G., and Naserabad, S. S. (2020). The protective effects of vitamin C on common carp (*Cyprinus carpio*) exposed to titanium oxide nanoparticles (TiO₂-NPs). *Aquaculture* 518, 734734. doi: 10.1016/j.aquaculture.2019.734734
- Hamed, S., El-Kassas, S., Abo-Al-Ela, H. G., Abdo, S. E., Abou-Ismail, U. A., and Mohamed, R. A. (2024). Temperature and feeding frequency: interactions with growth, immune response, and water quality in juvenile Nile tilapia. *BMC Veterinary Res.* 20, 520. doi: 10.1186/s12917-024-04366-4
- Hrubec, T. C., Cardinale, J. L., and Smith, S. A. (2000). Hematology and plasma chemistry reference intervals for cultured tilapia (Oreochromis hybrid). *Veterinary Clin. Pathol.* 29, 7–12. doi: 10.1111/j.1939-165X.2000.tb00389.x
- Hrubec, T. C., Smith, S. A., and Robertson, J. L. (2001). Age-Related Changes in Hematology and Plasma Chemistry Values of Hybrid Striped Bass (Morone chrysops × Morone saxatilis). *Veterinary Clin. Pathol.* 30, 8–15. doi: 10.1111/j.1939-165X.2001.tb00249.x
- Ji, K., Liang, H., Ren, M., Ge, X., Pan, L., and Yu, H. (2021). Nutrient metabolism in the liver and muscle of juvenile blunt snout bream (Megalobrama amblycephala) in response to dietary methionine levels. *Sci. Rep.* 11, 23843. doi: 10.1038/s41598-021-
- Jiang, X., Sun, F., Pan, Z., Xu, J., and Xie, S. (2024). Effects of dietary phytosterol on growth, lipid homeostasis and lipidomics of largemouth bass (Micropterus salmoides). *Aquaculture Rep.* 35, 101959. doi: 10.1016/j.aqrep.2024.101959
- Jiang, Y., Tao, Z., Chen, H., and Xia, S. (2021). Endoplasmic reticulum quality control in immune cells. Front. Cell Dev. Biol. 9, 740653. doi: 10.3389/fcell.2021.740653
 - Jobling, M. (1995). Fish bioenergetics. Oceanogr. Lit. Rev. 9, 785.
- Jobling, M. (2012). "National Research Council (NRC)," in *Nutrient requirements of fish and shrimp* (Springer, Washington, DC). The National Academies Press.
- Jovanović, B., Whitley, E. M., Kimura, K., Crumpton, A., and Palić, D. (2015). Titanium dioxide nanoparticles enhance mortality of fish exposed to bacterial pathogens. *Environ. pollut.* 203, 153–164. doi: 10.1016/j.envpol.2015.04.003
- Kaplan, A. (1984). "Urea," in Clin Chem The CV Mosby Co. Ed. L.A. Kaplan and A.J. Pesce (Princeton, USA: C.V. Mosby, St. Louis, MO), 1257–1260.
- Khan, S. K., Dutta, J., Ahmad, I., and Rather, M. A. (2024). Nanotechnology in aquaculture: Transforming the future of food security. *Food Chem. X* 24, 101974. doi: 10.1016/j.fochx.2024.101974
- Kim, J., Kundu, M., Viollet, B., and Guan, K.-L. (2011). AMPK and mTOR regulate autophagy through direct phosphorylation of Ulk1. *Nat. Cell Biol.* 13, 132–141. doi: 10.1038/ncb2152
- Kiser, M., Westerhoff, P., Benn, T., Wang, Y., Perez-Rivera, J., and Hristovski, K. (2009). Titanium nanomaterial removal and release from wastewater treatment plants. *Environ. Sci. Technol.* 43, 6757–6763. doi: 10.1021/es901102n
- Ko, J. A., and Hwang, Y. S. (2019). Effects of nanoTiO2 on tomato plants under different irradiances. *Environ. pollut.* 255, 113141. doi: 10.1016/j.envpol.2019.113141
- Kotil, T., Akbulut, C., and Yön, N. D. (2017). The effects of titanium dioxide nanoparticles on ultrastructure of zebrafish testis (*Danio rerio*). *Micron* 100, 38–44. doi: 10.1016/j.micron.2017.04.006
- Kozliak, E. I., and Paca, J. (2012). Journal of Environmental Science and Health, Part A. Toxic/hazardous substances and environmental engineering. Foreword. *J. Environ. Sci. Health Part A Toxic/hazardous Substances Environ. Eng.* 47, 919–919. doi: 10.1080/10934529.2012.667287
- Li, X., Xin, Y., Mo, Y., and Marozik, P. (2022). The bioavailability and biological activities of phytosterols as modulators of cholesterol metabolism. *Molecules* 27, 523. doi: 10.3390/molecules27020523

- Li, Y., Xu, J., Li, H., Xiao, X., Yang, X., Yi, C., et al. (2024). Based on network pharmacology and experimental validation: β-sitosterol inhibits cytokine storm by inducing autophagy. doi: 10.21203/rs.3.rs-4627381/v1
- Li, S. Q., Zhu, R. R., Zhu, H., Xue, M., Sun, X. Y., Yao, S. D., et al. (2008). Nanotoxicity of TiO(2) nanoparticles to erythrocyte in vitro. Food Chem. Toxicol. 46, 3626–3631. doi: 10.1016/j.fct.2008.09.012
- Liang, Q., Huang, Y., Zhu, N., Bei, Y., Shi, W., Chen, X., et al. (2024). Phytosterol supplementation enhances the growth performance, feed utilization, antioxidant status and glucose metabolism of juvenile largemouth bass (Micropterus salmoides) fed a high-starch diet. Front. Mar. Sci. Volume 11. doi: 10.3389/fmars.2024.1403563
- Liu, Z., Rui, M., and Yu, S. (2022). Occurrence of titanium dioxide nanoparticle in Taihu Lake (China) and its removal at a full-scale drinking water treatment plant. *Environ. Sci. pollut. Res.* 29, 23352–23360. doi: 10.1007/s11356-021-15775-5
- Livak, K. J., and Schmittgen, T. D. (2001). Analysis of relative gene expression data using real-time quantitative PCR and the 2(-Delta Delta C(T)) Method. *Methods* 25, 402–408. doi: 10.1006/meth.2001.1262
- Lopes-Virella, M. F., Stone, P., Ellis, S., and Colwell, J. A. (1977). Cholesterol determination in high-density lipoproteins separated by three different methods. *Clin. Chem.* 23, 882–884. doi: 10.1093/clinchem/23.5.882
- Luhata, L. P., and Usuki, T. (2021). Antibacterial activity of β -sitosterol isolated from the leaves of Odontonema strictum (Acanthaceae). *Bioorganic Medicinal Chem. Lett.* 48, 128248. doi: 10.1016/j.bmcl.2021.128248
- Lyu, S., Wei, X., Chen, J., Wang, C., Wang, X., and Pan, D. (2017). Titanium as a beneficial element for crop production. *Front. Plant Sci.* 8, 597. doi: 10.3389/fpls.2017.00597
- MaChado Kayser, J., Schuster, A., Zimmermann, G., Morisso, F., and Gehlen, G. (2022). Titanium dioxide nanoparticles promote histopathological and genotoxic effects in *Danio rerio* after acute and chronic exposures. *Nat. Sci.* 44, 1. doi: 10.5902/2179460X67963
- Maiga, D. T., Mamba, B. B., and Msagati, T. (2019). Distribution profile of titanium dioxide nanoparticles in South African aquatic systems. *Water Supply* 20, 516–528. doi: 10.2166/ws.2019.185
- McAndrew, B. J., Penman, D. J., Bekaert, M., and Wehner, S. (2016). "Tilapia genomic studies," in *Genomics in Aquaculture*, (The Netherlands: Elsevier, Amsterdam) 105–129. doi: 10.1016/B978-0-12-801418-9.00005-6
- Mihara, M., and Uchiyama, M. (1978). Determination of malonaldehyde precursor in tissues by thiobarbituric acid test. *Anal. Biochem.* 86, 271–278. doi: 10.1016/0003-2697(78)90342-1
- Min, Y., Suminda, G. G. D., Heo, Y., Kim, M., Ghosh, M., and Son, Y. O. (2023). Metal-based nanoparticles and their relevant consequences on cytotoxicity cascade and induced oxidative stress. *Antioxidants (Basel)* 12, 703. doi: 10.3390/antiox12030703
- Murray, R., and Kaplan, A. (1984a). "Alanine aminotransferase," in *Clinical Chemistry. Theory, analysis and correlation*. Eds. L. A. Kaplan and A. J. Pesce (MO, USA: CV Mosby St Louis), 1090.
- Murray, R., and Kaplan, A. (1984b). "Aspartate aminotransferase," in *Clinical Chemistry. Theory, analysis and correlation*. Eds. L. A. Kaplan and A. J. Pesce (MO, USA: CV Mosby Company), 1105–1108.
- Neiffer, D. L., and Stamper, M. A. (2009). Fish sedation, anesthesia, analgesia, and euthanasia: considerations, methods, and types of drugs. *ILAR J.* 50, 343–360. doi: 10.1093/ilar.50.4.343
- Nishikimi, M., Appaji Rao, N., and Yagi, K. (1972). The occurrence of superoxide anion in the reaction of reduced phenazine methosulfate and molecular oxygen. *Biochem. Biophys. Res. Commun.* 46, 849–854. doi: 10.1016/S0006-291X(72)80218-3
- Okamura, D., Araújo, F. G. D., Rosa, P. V. E., Freitas, R. T. F. D., Murgas, L. D. S., and Cesar, M. P. (2010). Effect of benzocaine concentration and fish size on anesthesia and recovery in Nile tilapia. *Rev. Bras. Zootecnia* 39, 971–976. doi: 10.1590/S1516-35982010000500005
- Paglia, D. E., and Valentine, W. N. (1967). Studies on the quantitative and qualitative characterization of erythrocyte glutathione peroxidase. *J. Lab. Clin. Med.* 70, 158–169.
- Perera, S., and Pathiratne, A. (2014). Haemato-immunological and histological responses in Nile tilapia, *Oreochromis niloticus* exposed to titanium dioxide nanoparticles. *Sri Lanka J. Aquat. Sci.* 17, 1–18. doi: 10.4038/sljas.v17i0.6852
- Ramalingam, S., Packirisamy, M., Karuppiah, M., Vasu, G., Gopalakrishnan, R., Gothandam, K., et al. (2020). Effect of β -sitosterol on glucose homeostasis by sensitization of insulin resistance via enhanced protein expression of PPR γ and glucose transporter 4 in high fat diet and streptozotocin-induced diabetic rats. Cytotechnology 72, 357–366. doi: 10.1007/s10616-020-00382-y
- Rashid, M. M., Forte Tavčer, P., and Tomšič, B. (2021). Influence of titanium dioxide nanoparticles on human health and the environment. *Nanomaterials (Basel)* 11, 2354. doi: 10.3390/nano11092354
- Rashid, H. O., Yadav, R. K., Kim, H. R., and Chae, H. J. (2015). ER stress: Autophagy induction, inhibition and selection. *Autophagy* 11, 1956–1977. doi: 10.1080/15548627.2015.1091141
- Reda, R. M., Zaki, E. M., Aioub, A. A. A., Metwally, M. M. M., Yassin, A. M., and Mahsoub, F. (2025). Behavioral, biochemical, immune, and histological responses of Nile tilapia (Oreochromis niloticus Linnaeus 1758) to lead, mercury, and

- pendimethalin exposure: individual and combined effects. *Environ. Sci. Europe* 37, 11. doi: 10.1186/s12302-024-01047-9
- Reyes-Becerril, M., Angulo, C., Cosío-Aviles, L., López, M. G., and Calvo-Gómez, O. (2022). Cylindropuntia cholla aqueous root rich in phytosterols enhanced immune response and antimicrobial activity in tilapia Oreochromis niloticus leukocytes. *Fish Shellfish Immunol.* 131, 408–418. doi: 10.1016/j.fsi.2022.10.028
- Ribeiro, L., Barbieri, E., and De Souza, A. (2025). Assessment of the toxicity of biosynthesized silver nanoparticles on Oreochromis niloticus (Nile tilapia). *Environ. Science: Nano* 12, 3173–3181. doi: 10.1039/D4EN01125B
- Rodríguez-González, V., Terashima, C., and Fujishima, A. (2019). Applications of photocatalytic titanium dioxide-based nanomaterials in sustainable agriculture. *J. Photochem. Photobiol. C: Photochem. Rev.* 40, 49–67. doi: 10.1016/j.jphotochemrev.2019.06.001
- Rojas-Hernandez, N., Véliz, D., and Vega-Retter, C. (2019). Selection of suitable reference genes for gene expression analysis in gills and liver of fish under field pollution conditions. *Sci. Rep.* 9, 3459. doi: 10.1038/s41598-019-40196-3
- Rook, G. A., Steele, J., Umar, S., and Dockrell, H. M. (1985). A simple method for the solubilisation of reduced NBT, and its use as a colorimetric assay for activation of human macrophages by gamma-interferon. *J. Immunol. Methods* 82, 161–167. doi: 10.1016/0022-1759(85)90235-2
- Sayed, A.E.-D.H., and Moneeb, R. H. (2015). Hematological and biochemical characters of monosex tilapia (Oreochromis niloticus, Linnaeus 1758) cultivated using methyltestosterone. *J. Basic Appl. Zoology* 72, 36–42. doi: 10.1016/j.jobaz.2015.03.002
- Sherif, A. H., Khalil, R. H., Tanekhy, M., Sabry, N. M., Harfoush, M. A., and Elnagar, M. A. (2022). Lactobacillus plantarum ameliorates the immunological impacts of titanium dioxide nanoparticles (rutile) in Oreochromis niloticus. *Aquaculture Res.* 53, 3736–3747. doi: 10.1111/are.15877
- Shi, C., Wu, F., and Xu, J. (2013). Incorporation of β -sitosterol into mitochondrial membrane enhances mitochondrial function by promoting inner mitochondrial membrane fluidity. *J. Bioenerg Biomembr* 45, 301–305. doi: 10.1007/s10863-012-9495-3
- Shi, D., Zhou, L., Shi, H., Zhang, J., Zhang, J., Zhang, L., et al. (2023). Autophagy is induced by swine acute diarrhea syndrome coronavirus through the cellular IRE1-JNK-Beclin 1 signaling pathway after an interaction of viral membrane-associated papain-like protease and GRP78. *PloS Pathog.* 19, e1011201. doi: 10.1371/journal.ppat.1011201
- Siqueira, P. R., Carmo, T. L. L. D., Bonomo, M. M., Santos, F., and Fernandes, M. N. (2021). Proliferative response avoids mutagenic effects of titanium dioxide (TiO₂) nanoparticles in a zebrafish hepatocyte cell line. *J. Hazard. Mater. Adv.* 4, 100036. doi: 10.1016/j.hazadv.2021.100036
- Siwicki, A. K., Anderson, D. P., and Rumsey, G. L. (1994). Dietary intake of immunostimulants by rainbow trout affects non-specific immunity and protection against furunculosis. *Vet. Immunol. Immunopathol.* 41, 125–139. doi: 10.1016/0165-2427(94)90062-0
- Smith, M., and Wilkinson, S. (2017). ER homeostasis and autophagy. *Essays Biochem.* 61, 625–635. doi: 10.1042/EBC20170092
- Song, Y., Lu, Z., Zhang, X., Xu, J., Gong, M., Meng, L., et al. (2022). Dietary β-sitosterol supplementation enhanced intestinal immune function of large yellow croaker (*Larimichthys crocea*) infected with *Aeromonas hydrophila*. *Aquac. Res.* 53, 6545–6561. doi: 10.1111/are.16123
- Soror, E. I., El Asely, A. M., Abdel Gawad, E. A., Radwan, H. A., and Abbass, A. A. (2021). Recuperative effects of honey bee pollen, ginger (Zingiber officinale), and Moringa oleifera in Nile tilapia (Oreochromis niloticus L.) after sub-lethal exposure to dimethoate. *Aquaculture* 530, 735886. doi: 10.1016/j.aquaculture.2020.735886
- Souza, R., Campeche, D., Campos, R., Figueiredo, R., and Melo, J. (2014). Feeding frequency for tambaqui juveniles. *Arquivo Brasileiro Med. Veterinária e Zootecnia* 66, 927–932. doi: 10.1590/1678-41625557
- Sreedharan, S. P., Kumar, A., and Giridhar, P. (2018). Primer design and amplification efficiencies are crucial for reliability of quantitative PCR studies of caffeine biosynthetic N-methyltransferases in coffee. 3 *Biotech.* 8, 467. doi: 10.1007/s13205-018-1487-5
- Sungur, Ş. (2021). "Titanium dioxide nanoparticles," in *Handbook of nanomaterials and nanocomposites for energy and environmental applications*, (Switzerland: Springer, Cham) 713–730. doi: 10.1007/978-3-030-36268-3_9
- Suvarna, K. S., Layton, C., and Bancroft, J. D. (2018). Bancroft's theory and practice of histological techniques. (Philadelphia, PA, USA: Elsevier health sciences).
- Tang, X., Yan, T., Wang, S., Liu, Q., Yang, Q., Zhang, Y., et al. (2024). Treatment with β -sitosterol ameliorates the effects of cerebral ischemia/reperfusion injury by suppressing cholesterol overload, endoplasmic reticulum stress, and apoptosis. Neural. Regen. Res. 19, 642–649. doi: 10.4103/1673-5374.380904
- Tang, T., Zhang, Z., and Zhu, X. (2019). Toxic effects of TiO2 NPs on zebrafish. *Int. J. Environ. Res. Public Health* 16, 523. doi: 10.3390/ijerph16040523
- Tunçsoy, M. (2021). Impacts of titanium dioxide nanoparticles on serum parameters and enzyme activities of Clarias gariepinus. *Bull. Environ. Contamination Toxicol.* 106, 629–636. doi: 10.1007/s00128-020-03100-8
- Uribe-García, A., Medina-Reyes, E. I., Flores-Reyes, C. A., Zagal-Salinas, A. A., Ispanixtlahuatl-Meraz, O., Delgado-Armenta, E., et al. (2025). Food grade titanium dioxide induced endoplasmic reticulum stress in colon cells: Comparison between normal and colorectal carcinoma cells. *Toxicol. Vitro* 102, 105957. doi: 10.1016/j.tiv.2024.105957

Vasantharaja, D., Ramalingam, V., and Reddy, G. A. (2015). Titanium dioxide nanoparticles induced alteration in haematological indices of adult male wistar rats. *J. Acad. Ind. Res.* 3, 632–635.

Vignardi, C. P., Hasue, F. M., Sartório, P. V., Cardoso, C. M., MaChado, A. S. D., Passos, M., et al. (2015). Genotoxicity, potential cytotoxicity and cell uptake of titanium dioxide nanoparticles in the marine fish *Trachinotus carolinus* (Linnaeus 1766). *Aquat. Toxicol.* 158, 218–229. doi: 10.1016/j.aquatox.2014.11.008

Vineetha, V. P., Devika, P., Prasitha, K., and Anilkumar, T. V. (2021). *Tinospora cordifolia* ameliorated titanium dioxide nanoparticle-induced toxicity via regulating oxidative stress-activated MAPK and NRF2/Keap1 signaling pathways in Nile tilapia (*Oreochromis niloticus*). *Comp. Biochem. Physiol. C: Toxicol. Pharmacol.* 240, 108908. doi: 10.1016/j.cbpc.2020.108908

Weinert, N. C., Volpato, J., Costa, Á., Antunes, R. R., Oliveira, A. C. D., Mattoso, C. R. S., et al. (2015). Hematology of Nile tilapia (Oreochromis niloticus) subjected to anesthesia and anticoagulation protocols. *Semina: Ciências Agrárias* 36, 4237–4250. doi: 10.5433/1679-0359.2015v36n6Supl2p4237

Wenger, C., Kaplan, A., Rubaltelli, F., and Hammerman, C. (1984). Alkaline phosphatase. Kaplan A et al. Clin Chem The C.V. Mosby Co. St Louis. Toronto. Princeton, 1094–1098.

Zahran, E., Abdelhamid, F., Aboelfadl, E., and El-Matbouli, M. (2021). Biomarker responses of Nile tilapia towards wastewater effluents exposure. *Aquaculture Res.* 52, 1382–1394. doi: 10.1111/are.14992

Zhang, X., Liu, B., Lal, K., Liu, H., Tran, M., Zhou, M., et al. (2023). Antioxidant system and endoplasmic reticulum stress in cataracts. $Cell\ Mol.\ Neurobiol.\ 43,\ 4041-4058.\ doi: 10.1007/s10571-023-01427-4$

Zhou, Z., Liu, T., Kong, J., Zhao, Z., and Zhu, J. (2024). Combined proteomic and metabolomic studies on the liver of Amur sturgeon Acipenser schrenckii under titanium dioxide nanoparticle exposure. *J. Oceanology Limnology* 42, 1001–1015. doi: 10.1007/s00343-023-3137-y

Zhou, Z., Zhu, J., Zheng, X., Luo, T., and Lv, S. (2025). Derlin-1 modulated endoplasmic reticulum stress and apoptosis in Acipenser schrenckii hepatocytes under titanium dioxide nanoparticle exposure. *Aquat. Toxicol.* 286, 107467. doi: 10.1016/j.aquatox.2025.107467